

## PHYSICAL CHARACTERISTICS OF THE RR LYRAE STARS IN THE VERY METAL POOR GLOBULAR CLUSTER NGC 5053

JAMES M. NEMEC<sup>1</sup>

International Statistics and Research Corporation, P.O. Box 496, Brentwood Bay, BC V8M 1R3, Canada; jmn@isr.bc.ca

Received 2003 October 8; accepted 2004 January 13

### ABSTRACT

The physical characteristics of the 10 RR Lyrae stars in the very metal-poor globular cluster NGC 5053 are derived from photometry of  $\sim 1000$   $B$  and  $V$  CCD frames acquired from 1994 to 2002 with the Dominion Astrophysical Observatory 1.8 m Plaskett Telescope. Revised pulsation periods and light curves, mean magnitudes, colors, amplitudes, and Fourier parameters are presented. Periods accurate to  $\leq 10^{-5}$  days are now known for all 10 RR Lyrae stars. Using times of maximum light dating back to Baade's original 1923–1927 observations, period change rates,  $dP/dt$ , accurate to  $\leq 0.07$  days  $\text{Myr}^{-1}$ , have been derived for the 10 stars. Seven stars have increasing periods, and three have decreasing periods, with the estimated period change rates for V1, V2, V9, and V10 being very close to zero. The mean  $dP/dt$  is equal to  $0.04 \pm 0.04$  days  $\text{Myr}^{-1}$  and is consistent with Lee's evolutionary model predictions for a cluster with horizontal-branch type  $\sim 0.5$ . Mean  $B-V$  colors range from 0.20 to 0.40 and are more consistent with near-zero reddening than alternative higher estimates. A reddening  $E_{B-V} = 0.018 \pm 0.003$  is derived from the 1998 SFD maps. Mean effective temperatures vary from 6040 K (V10) to 7290 K (V6), with  $2.6 \leq \log g \leq 3.1$ . Visual and bolometric absolute magnitudes, bolometric corrections, and luminosities are derived using Fourier methods and using intensity- and magnitude-averaged mean magnitudes. Mean locations of the stars in the H-R diagram tend to progress from hotter, lower  $L$  stars to cooler, higher  $L$  stars and are consistent with theoretical blue and red edges of the instability strip. Masses estimated assuming zero reddening and Dorman's oxygen-enhanced models range from  $0.68 M_{\odot}$  (V6) to  $0.78 M_{\odot}$  (V10) for the 10 stars. The mean metal abundance for NGC 5053 derived using the Jurcsik-Kovács method lies significantly higher than the range  $-2.3$  to  $-2.6$  dex determined using other, more well established methods. This finding supports recent suggestions that metallicities derived from Fourier-based  $[\text{Fe}/\text{H}]$  calibrations need to be revised downward by at least 0.3 dex for RR Lyrae stars with very low metal abundances.

*Key words:* globular clusters: individual (NGC 5053) — RR Lyrae variable — stars: abundances — stars: distances — stars: evolution — stars: horizontal-branch

*On-line material:* machine-readable tables

### 1. INTRODUCTION

In 1928, Walter Baade (1928) reported the discovery of nine RR Lyrae stars in the globular cluster NGC 5053 (C1313+179); a tenth RR Lyrae star was subsequently discovered by Helen Sawyer (1946). Today NGC 5053 is best known for its very low central concentration,  $\log(r_i/r_c) = 0.75$  (King 1962), its extremely low metal abundance,  $[\text{Fe}/\text{H}] \sim -2.5$  dex (Zinn & West 1984; Sarajedini & Milone 1995; Sohn 2001), and its significant population of  $\sim 25$  blue stragglers (Nemec & Cohen 1989; Sarajedini & Milone 1995), five of which are very short period (49 minutes  $\leq P \leq 57$  minutes) SX Phoenicis stars with very low luminosities ( $3.0 \leq M_V \leq 3.3$ ) and small amplitudes,  $0.08 \text{ mag} \leq A_V \leq 0.25 \text{ mag}$  (Nemec & Mateo 1990; Nemec et al. 1995). The low metallicity of the cluster undoubtedly explains the long mean period of the RRab stars, 0.690 days (Nemec, Mateo, & Schombert 1995), and may also account for the extreme properties of the SX Phe stars. Because NGC 5053 contains both RR Lyrae and SX Phe stars, it has proved useful for calibrating the period-luminosity relations of Population II variable stars (Nemec, Linnell Nemec, & Lutz 1994).

The purpose of the present paper is to establish the period change rates and other fundamental properties of the RR Lyrae

stars in this most metal-poor globular cluster and to use these quantities to improve our understanding of their physical characteristics and evolution.

In § 2, the CCD observations are described and new  $B$ ,  $V$  photometry is presented. Pulsation periods, light curves, and photometric characteristics of the RR Lyrae stars are given in § 3, and in § 4 period change rates are derived using all available photometry since 1923. The latter estimates are important because theoretical models, such as those of Lee (1991), predict that the period change rates of RR Lyrae stars vary with horizontal-branch (HB) type. In § 5, Fourier decomposition coefficients and associated parameters are derived from  $V$  and  $B$  light curves and are used to compute various physical characteristics, which are compared with values computed by other means. These characteristics of the individual RR Lyrae stars include mean  $B-V$  colors and  $E_{B-V}$  reddenings (§ 6), surface gravities and effective temperatures (§ 7), visual and bolometric absolute magnitudes and luminosities (§ 8), masses (§ 9), and metal (and helium) abundances (§ 10). The paper concludes with a summary of the main results (§ 11).

### 2. OBSERVATIONS

Between 1994 and 2002, the Dominion Astrophysical Observatory 1.8 m (72 inch) Plaskett Telescope was used at regular intervals to acquire CCD images of NGC 5053

<sup>1</sup> Guest investigator, Dominion Astrophysical Observatory, Herzberg Institute of Astrophysics, National Research Council of Canada.

TABLE 1  
CCD OBSERVATIONS OF NGC 5053

Night	HJD Range (2,400,000+)	CCD Camera	$N(B)$	$N(V)$	RR Lyrae Stars Observed
1994 Mar 14/15 .....	49,426.79–0.85	Tek-2	4	9	V2–V8, V10
1994 Apr 9/10.....	49,452.75–0.03	SITe-1	23	29	V1–V4, V6–V10
1994 May 5/6 .....	49,478.69–0.93	SITe-1	19	30	V1–V8, V10
1994 May 6/7 .....	49,479.70–0.98	SITe-1	2	17	V1–V8, V10
1994 May 7/8 .....	49,480.74–0.99	SITe-1	0	42	V1–V10
1995 Feb 28/Mar 1 .....	49,777.80–0.09	SITe-1	13	19	V1–V10
1995 Mar 1/2 .....	49,778.81–0.08	SITe-1	8	11	V1–V10
1995 Mar 2/3 .....	49,779.82–0.08	SITe-1	8	11	V1–V10
1995 Mar 28/29.....	49,805.73–0.02	SITe-1	11	12	V1–V10
1995 Mar 29/30.....	49,806.73–0.03	SITe-1	8	10	V2–V4, V6–V8, V10
1995 Mar 30/31.....	49,807.78–0.81	SITe-1	1	2	V2–V4, V6, V8, V10
1995 Apr 23/24.....	49,831.69–0.00	SITe-1	6	8	V1–V10
1995 Apr 24/25.....	49,832.69–0.99	SITe-1	5	6	V1–V10
1995 Apr 25/26.....	49,833.74–0.89	SITe-1	3	3	V1–V10
1997 Apr 3/4.....	50,542.87–0.88	SITe-3	1	1	V2–V4, V6–V10
1999 Apr 16/17.....	51,285.77–0.83	SITe-5	0	3	V2–V4, V6–V8, V10
1999 Apr 18/19.....	51,287.70–0.92	SITe-5	14	41	V1–V4, V6–V10
1999 Jun 11/12.....	51,341.77–0.81	SITe-5	1	8	V1–V4, V6–V10
1999 Jun 13/14.....	51,343.77–0.85	SITe-5	21	23	V1–V4, V6–V10
2000 Mar 4/5 .....	51,608.81–0.07	SITe-5	7	55	V1–V4, V6–V10
2000 Mar 5/6 .....	51,609.78–0.08	SITe-5	8	60	V1–V4, V6–V10
2000 May 7/8 .....	51,672.71–0.87	SITe-5	5	25	V1–V4, V6–V10
2000 Jun 1/2 .....	51,697.74–0.77	SITe-5	3	4	V2–V8, V10
2001 May 19/20.....	52,049.80–0.96	SITe-5	14	15	V2–V3, V5–V10
2001 May 20/21.....	52,050.73–0.95	SITe-5	11	39	V2–V8, V10
2001 May 21/22.....	52,051.73–0.94	SITe-5	6	37	V2–V8, V10
2001 May 22/23.....	52,052.75–0.93	SITe-5	15	26	V2–V8, V10
2001 Jun 22/23.....	52,083.75–0.80	SITe-5	2	8	V2–V8, V10
2001 Jun 25/26.....	52,086.74–0.82	SITe-5	2	16	V2–V8, V10
2002 Feb 15/16.....	52,321.83–0.92	SITe-5	2	12	V1–V4, V6–V10
2002 May 1/2 .....	52,396.69–0.88	SITe-5	3	35	V2–V5, V7–V10
2002 May 8/9 .....	52,403.69–0.95	SITe-5	19	45	V1–V10
2002 May 9/10.....	52,404.70–0.96	SITe-5	11	57	V1–V10
2002 May 10/11.....	52,405.80–0.96	SITe-5	12	24	V1–V10

( $\alpha = 13^{\text{h}}16^{\text{m}}6, \delta = +17^{\circ}41'$ , epoch 2003.5). The  $9' \times 9'$  field of view of the imaging CCD camera and mean  $V$  magnitude of the RR Lyrae stars  $\sim 16.6$  (Nemec et al. 1995) make NGC 5053 well suited for spring and early summer observations. A summary of the observations is given in Table 1.

Four generations of cameras were used, all of which had a array size of  $1024 \times 1024$  pixels, each pixel having a size of  $24 \mu\text{m}$ , with readout noise  $\sim 12 e^- \text{ pixel}^{-1}$  and gain  $\sim 5 e^- \text{ ADU}^{-1}$ . Owing to the limited field of view, not all 10 stars could be captured on a single frame; therefore, on some nights the telescope was shifted northwest and southeast, and on other occasions only a subset of the stars were observed. A total of almost a thousand frames (727  $V$  frames, 268  $B$  frames) were taken and photometrically measured. In general, the exposure times were 5 minutes for the  $V$  frames and 10 minutes for the  $B$  frames. Dawn and dusk sky flats were median-filtered and used to obtain average  $B$  and  $V$  sky flats for each night. Bias frames, taken before and during the night, and the over-scan regions of individual frames, were used to correct for bias. Unusable pixels were trimmed from all frames. The seeing was never better than  $1''$ , but for this very open globular cluster (concentration class XII) the sizes of the stellar images were not critical, even in the case of V4, which is crowded by a neighboring star of similar magnitude.

Instrumental magnitudes were measured for individual stars with the IRAF version of the CCD point-spread function

photometry program DAOPHOT (Stetson 1987). These were calibrated using a combination of the photometry published by Sandage, Katem, & Johnson (1977) and Nemec et al. (1995). The photometry in both studies is consistent with the CCD photometry of Sarajedini & Milone (1995).

The calibrated  $V$  and  $B$  magnitudes for the RR Lyrae stars are given in Tables 2 and 3. The first column of each table contains the Heliocentric Julian Date (HJD) of the observation, where the mid-exposure HJD was computed using the SETJD command in IRAF. The other columns contain the magnitudes. The range of the  $V$  and  $B$  magnitudes of the RR Lyrae stars is  $16\text{--}17.5$  mag, with uncertainties in the individual measurements typically  $\lesssim 0.01$  mag.

### 3. PULSATION PERIODS, LIGHT CURVES, AND PHOTOMETRIC CHARACTERISTICS

Pulsation periods for Baade's nine RR Lyrae stars are well established from the work of Sawyer (1946), Rosino (1949), Mannino (1963), and Nemec et al. (1995). Comparison of these periods in Table 4 shows that the periods derived by Sawyer for V1, V2, V3, V6, V7, V8, and V9 agree with later estimates to within  $\sim 1/1000$ th of a day ( $\sim 1.4$  minutes), while the periods for the longer period stars, V4 and V5, were first established by Rosino, and then confirmed by Mannino.

No reliable estimate of the period for Sawyer's variable, V10, was available prior to the present study, although its  $P$

TABLE 2  
JOHNSON  $V$  PHOTOMETRY OF THE NGC 5053 RR LYRAE STARS (1994–2002)

HJD (2,400,000+)	V1	V2	V3	V4	V5	V6	V7	V8	V9	V10
1994 Mar 14/15:										
49,426.7903.....	...	16.854	16.713	15.873	...	16.388	16.335	15.117	...	16.623
49,426.7959.....	...	16.860	16.766	...	...	16.488	16.336	15.282	...	16.590
49,426.8014.....	...	16.899	16.677	...	...	16.510	16.344	15.249	...	16.739
49,426.8063.....	...	16.935	16.782	16.087	16.374	16.434	16.335	15.329	...	16.760

NOTE.—Table 2 is presented in its entirety in the electronic edition of the *Astronomical Journal*. A portion is shown here for guidance regarding its form and content.

was thought to be longer than 0.6 days by Nemeč et al. (1995). To remedy this situation, as well as provide a check of the periods of the other variable stars, period searches of the new photometry were made using the Lafler & Kinman (1965) phase dispersion minimization method. One of the period searches for V10 is illustrated in Figure 1, where the adopted period  $P = 0.775851$  days (epoch 1995–2002) is seen to be highly significant. Significantly shorter periods are ruled out by real-time light curves.

$V$  and  $B$  light curves for the 10 stars are plotted in Figure 2. To facilitate comparisons the same scale has been used for all figures. Each graph is labeled with the assumed period,  $P$ , and the assumed time of zero phase,  $T_0$ . These same values were used in the period change study to plot the photometry from all the epochs (but are not necessarily the final adopted periods). The light curves include only photometry from those epochs that best illustrate the shapes of the light curves, and the epochs of the plotted data are recorded on each graph. The inclusion of additional photometry would have resulted in varying degrees of “phase smearing,” depending on the period change rate. Notes on the individual stars are given in the Appendix.

In Table 5 the photometric characteristics derived from the light curves are summarized. Magnitudes at maximum light,  $V(\max)$  and  $B(\max)$ , and the max-to-min amplitudes,  $A_V$  and  $A_B$ , were read directly from Figure 2. Two types of mean magnitudes were calculated for both  $\langle V \rangle$  and  $\langle B \rangle$ : intensity-averaged (int) values and magnitude-averaged (mag) values, both of which were derived from the Fourier fitting procedure. (The  $A_V$  and  $A_B$  are equivalent to  $A_V(0)$  and  $A_B(0)$  in the header of Table 9 below). The uncertainties in the mean magnitudes and amplitudes are typically  $\pm 0.01$  in  $V(\max)$  and  $B(\max)$ , and  $\pm 0.02$  in  $A_V$  and  $A_B$ . The uncertainty in the  $\langle V \rangle$  is generally less than in the  $\langle B \rangle$  (compare the  $\sigma_V$  and  $\sigma_B$  in Table 9). The ensemble mean values,  $\langle V \rangle_{\text{int,all}} = 16.60 \pm 0.03$  (col. [6]) and  $\langle V \rangle_{\text{mag,all}} = 16.62 \pm 0.03$  (col. [7]), are in good

agreement with previously derived magnitude levels of the HB:  $V(\text{HB}) = 16.63$  (Sandage et al. 1977),  $16.65 \pm 0.03$  (Sarajedini & Milone 1995), and  $16.67 \pm 0.07$  (Sohn 2001).

Color curves (around the light cycles) are plotted in Figure 3, which also shows the intensity-mean  $V$  magnitudes and  $\langle B \rangle - \langle V \rangle$  colors of the stars. The four RRc stars are the hottest of the RR Lyraes, while the six  $ab$ -type stars are cooler and tend to be more luminous. Apart from V7, which has a high luminosity for its color (possibly owing to advanced evolution), the RR Lyrae stars tend to be hottest (bluest) when they are most luminous and coolest when they are least luminous. The observed rate of dimming with cooling is similar for all the stars and is estimated to be  $dV/d(B-V) \sim 3.2$ . In general, the RRc stars and the longest period RRab stars exhibit smaller temperature and luminosity ranges (i.e., smaller loops) than the shortest period RRab stars, which is not unusual.

Figure 4 is a color-magnitude diagram for NGC 5053 showing the mean positions of the RR Lyrae stars and the brightest stars (as defined by the photometry of Sarajedini & Milone 1995). The intensity-mean magnitudes and colors of the RR Lyrae stars clearly place them between the red and blue HB stars. Schematic blue and red edges of the instability strip are also depicted in Figure 4; these occur at  $B-V = 0.18 \pm 0.02$  and  $0.41 \pm 0.01$ , respectively. These colors are similar to the blue and red edges at  $(B-V)_0 = 0.17$  and  $0.38$  for the variable stars in M15 (see Fig. 7 of Sandage 1990) and suggest for NGC 5053 a very small or negligible reddening.

#### 4. PERIOD CHANGE RATES

Attempts to derive period change rates for the NGC 5053 stars were made previously by Sawyer (1946), Mannino (1963), and Nemeč et al. (1995). While these authors were able to say that the periods for several of the stars probably are changing, in general the results of their  $dP/dt$  determinations were not successful, owing mainly to the short time interval of the observations then available. With the new photometry and

TABLE 3  
JOHNSON  $B$  PHOTOMETRY OF THE NGC 5053 RR LYRAE STARS (1994–2002)

HJD (2,400,000+)	V1	V2	V3	V4	V5	V6	V7	V8	V9	V10
1994 Mar 14/15:										
49,426.8223.....	...	17.153	16.838	16.813	16.634	16.721	16.473	16.010	...	16.994
49,426.8327.....	...	17.242	16.769	16.838	16.521	16.811	16.522	16.080	...	17.089
49,426.8431.....	...	17.251	16.669	16.826	16.478	16.870	16.545	16.088	...	16.989
49,426.8535.....	...	17.256	16.534	...	16.348	16.817	...	...	...	...

NOTE.—Table 3 is presented in its entirety in the electronic edition of the *Astronomical Journal*. A portion is shown here for guidance regarding its form and content.

TABLE 4  
PREVIOUSLY DERIVED PERIODS AND PERIOD CHANGE RATES

STAR (1)	SAWYER 1946		ROSINO 1949	MANNINO 1963		NEMEC ET AL. 1995	
	$P_S$ (days) (2)	$\beta$ (days Myr $^{-1}$ ) (3)	$P_R$ (days) (4)	$P_M$ (days) (5)	$\beta$ (days Myr $^{-1}$ ) (6)	$P_N$ (days) (7)	$\beta$ (days Myr $^{-1}$ ) (8)
V1.....	0.647178		0.647178	0.6471748		0.647194:	$\neq 0$
V2.....	0.378953		0.378953	0.3789561	0.16	0.378956	(0.16)
V3.....	0.592946		0.592946	0.5929430		0.592947	
V4.....	0.400585		0.667061	0.6670627		0.667073	0.33
V5.....	0.416868		0.714861	0.7148605		0.71486	
V6.....	0.292198		0.292199	0.2921978		0.292188	-0.39
V7.....	0.351581		0.351581	0.3519300	0.50	0.351943	(0.50)
V8.....	0.362842	-0.44	0.362845	0.3628410	(-0.40)	0.362603	(-0.40)
V9.....	0.74173	1.75	0.741741	0.7402201		0.740220	(1.75)
V10.....	0.30354		0.437397	0.4373803		$\geq 0.6$	

the almost 80 yr interval since Baade's first observations, the present investigation largely overcomes this problem and has led to period change rates with relatively small uncertainties, in the range  $\pm 0.02$  to  $\pm 0.07$  days Myr $^{-1}$ .

The methods used for deriving the period change rates were the same as those described in detail by Nemeč, Hazen-Liller, & Hesser (1985). Light curves were plotted for each epoch using the available photometry and the assumed  $P$  (days) and epoch of maximum light,  $T_0$ , given in Table 6. The same table contains the mean HJD for each epoch and the measured phases of maximum light (with associated uncertainties).

Figure 5 shows the phase-shift diagrams for the NGC 5053 RR Lyraes. The phases of maximum light are those representing the photometric observations made between 1924 and 2002, with error bars corresponding to the estimated uncertainties. Owing to the possibility of the loss of cycle counts, there was some subjectiveness in the adopted phases of maximum light, but in general such problems were minimal because there was enough data and enough phase coverage that the variations were smooth. Several possibilities were evaluated for the shortest period RRc stars V6, V7, and V8, two of which have been plotted for V7. The phases for V7 given in Table 6 correspond to the  $dP/dt = +0.95$  days

Myr $^{-1}$  solution; for the  $-0.28$  days Myr $^{-1}$  solution, one simply adjusts the phases upward or downward by an integer to obtain the configuration shown in Figure 5.

The parabolas and straight lines in Figure 5 were derived from weighted least-squares fits to the phases. The parabolas correspond to the fitting of a second-order polynomial, i.e.,  $y = a + bx + cx^2$ , with weights determined using the errors in the phases of maximum light. The results of the fits are summarized in Table 7. The coefficients of the quadratic curves are given in columns (4)–(6), along with the error estimates. The root mean square error of the fit,  $\sigma_{\text{rms}}$ , and the  $R^2$  goodness-of-fit statistic<sup>2</sup> are recorded in columns (7) and (8). The number of epochs used for the fit is given in column (9), and column (10) contains the epoch,  $E$ , at which the parabola is an extremum, i.e., the epoch at which the assumed period is applicable, computed using  $E = -b/(2c^2)$ . The last column contains the derived period change rate,  $\beta \equiv dP/dt = 2cP^2$ . The formal uncertainty derived from the least-squares fit depends mainly on the error in  $c$ . The uncertainties were found at worst to be  $\pm 0.07$  days Myr $^{-1}$ . Both increasing and decreasing period changes were found, ranging from  $dP/dt = -0.32$  days Myr $^{-1}$  for V6 to  $+0.48$  days Myr $^{-1}$  for V8. For V7,  $\beta = +0.95 \pm 0.10$  days Myr $^{-1}$  is a possibility, but is less likely than  $-0.28 \pm 0.04$  days Myr $^{-1}$ . While it is recognized that the “ $O-C$  diagrams for RR Lyrae stars can differ greatly from parabolas” (Smith 1995) parabolic (or linear) fits seem reasonable for all the NGC 5053 RR Lyrae stars.

For those stars where the curvature of the fitted parabola is less than  $0.20$  days Myr $^{-1}$ , the data were also fitted with a straight line. The resulting coefficients of the line,  $y = a + bx$ , and measures of the weighted least squares fit,  $\sigma_{\text{rms}}$  and  $R^2$ , are given in Table 8. A positive slope in Figure 5 indicates that the true period is larger than the assumed period. For example, the true period for V1 is larger than the assumed period by  $0.000014$  days ( $=bP^2$ ). A negative slope (e.g. V2, V4, V9, and V10) suggests a smaller true period. The resulting best estimate of the period, if  $P$  is indeed constant, is given in the last column of Table 8. As one can see, the derived “true” periods agree well with the previously derived periods but are now 10 to 100 times more precise, with uncertainties smaller than  $\pm 4 \times 10^{-7}$  days (or less than  $\pm 4/100$ ths of a second).

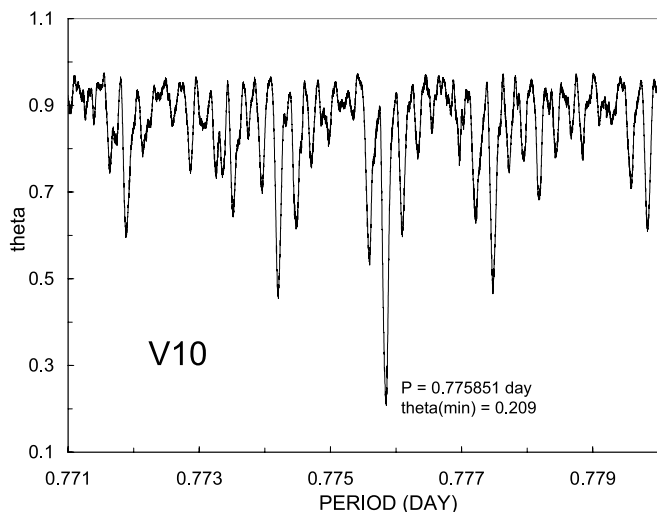


FIG. 1.—Period search for V10, whose period previously was not known. This phase dispersion minimization diagram, which is based on all the  $V$  photometry, shows that the most probable period is 0.775851 days.

<sup>2</sup> The coefficient of determination,  $R^2$ , is the proportion of the total variation explained by the polynomial (or linear) fit. The closer the value is to 1.0 the better is the statistical measure of the fit.

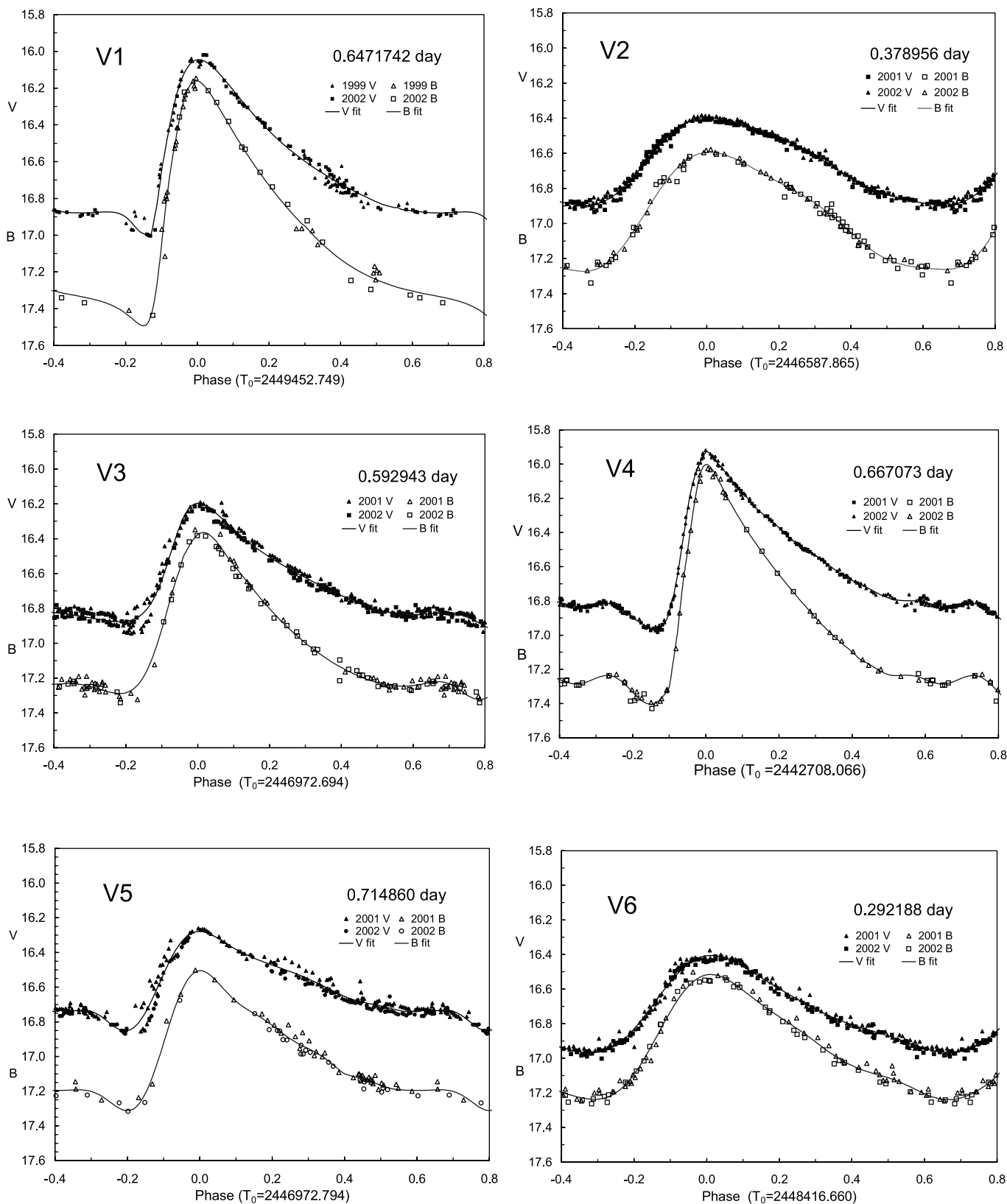


FIG. 2.—*V* (top) and *B* (bottom) light curves for the ten RR Lyrae stars in NGC 5053. For each star, the phases range from  $-0.4$  to  $0.8$ , the magnitudes range from  $15.8$  to  $17.6$ , and phase shifts necessary for the maximum to occur at phase =  $0$  have been applied (e.g., for V1 the 1999 photometry have been phase-shifted  $-0.06$  and the 2002 photometry has been phase-shifted  $+0.07$ ).

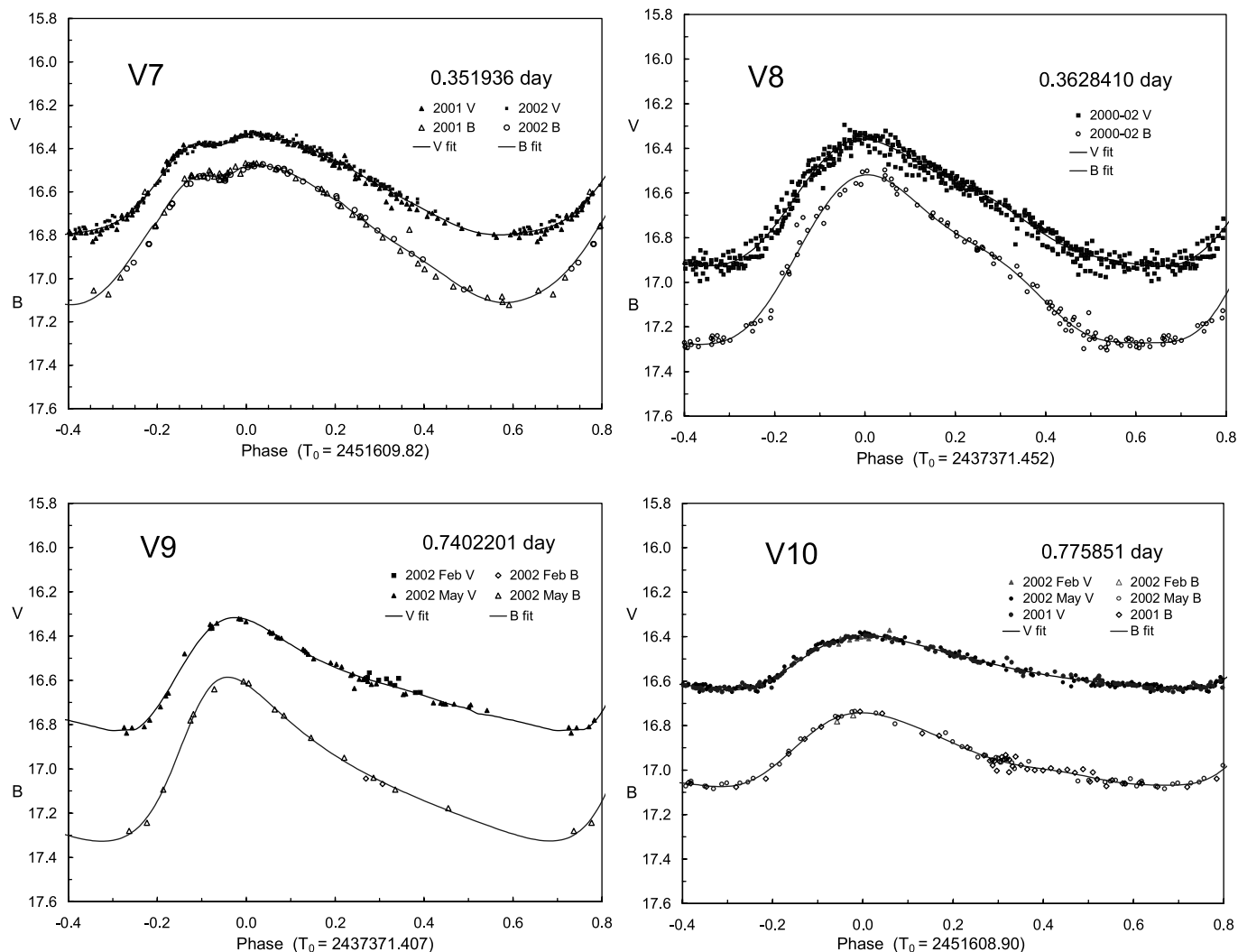


FIG. 2.—Continued

Having considered the possibility of a constant period, and the possibility of a changing period, it remained to make a final decision as to the long-term periodic behavior of each star. For this decision  $p$ -values<sup>3</sup> were computed for the “ $c$ ” coefficients of the quadratic fits. These were found to be useful since they measure the probability that  $c$  is very near to zero. For V3 to V8, the  $p$ -values are near zero, and it can be concluded that these stars almost certainly are changing their periods. The  $p$ -values for V1, V2, V9, and V10 are 0.45, 0.77, 0.29, and 0.72, respectively, from which it is concluded that the period change rates for these four stars, all of which have very small “derived” period change rates, could, quite possibly, be zero.

How well do the derived period change rates compare with the previously derived period change rates given in Table 4? As noted above, the previous rates are less reliable because of the much shorter time baseline. Comments on specific stars are given in the Appendix.

Figure 6 shows a histogram of the period change rates for the 10 RR Lyrae stars in NGC 5053. Also shown is a normal

<sup>3</sup> The  $p$ -value is the probability that the estimated  $c$  has a magnitude at least as large as the observed value when the true  $c$  is zero (i.e., no curvature). It is a measure of the statistical significance of the curvature exhibited by the current sample.

distribution with mean period change rate of  $0.041 \text{ days Myr}^{-1}$  and standard deviation  $0.247 \text{ days Myr}^{-1}$ . With a total uncertainty for the mean of  $\pm 0.04 \text{ days Myr}^{-1}$  a mean of zero is a distinct possibility.

Figure 7 is a color-magnitude diagram for NGC 5053 in the instability strip region of the HB. It is patterned after Figure 10 of Iben & Rood (1970) and Figure 2 of Smith & Sandage (1981), wherein the lengths of the vectors are proportional to  $dP/dt$ , with vectors up and to the right corresponding to increasing periods, and vectors down and to the left corresponding to decreasing periods. For the four stars with very small (or nil) period change rates (V1, V2, V9, and V10) the vectors were too short to be plotted. The only apparent pattern is that the short-period RR Lyrae stars have the greatest period change rates. There is no pattern relative to the theoretical HB tracks (see below). Thus, it can be concluded, as was found previously by Iben & Rood (1970) for M3, by Nemeč et al. (1985) for NGC 2257 in the Large Magellanic Cloud, and by others (Lee 1991), that the measured  $dP/dt$  rates do not seem to reflect stellar evolution as a result of nuclear burning, but probably are caused by some other effect.

Figure 8 is a plot of HB type, defined as  $(B-R)/(B+V+R)$  by Lee (1990), against mean (or median) period change rate,  $dP/dt$ , for the RR Lyrae stars in many different globular

TABLE 5  
PHOTOMETRIC CHARACTERISTICS OF THE NGC 5053 RR LYRAE STARS

Star (1)	RR Type (2)	$P$ (days) (3)	$V(\max)$ (4)	$A_V$ (5)	$\langle V \rangle_{\text{int}}$ (6)	$\langle V \rangle_{\text{mag}}$ (7)	$B(\max)$ (8)	$A_B$ (9)	$\langle B \rangle_{\text{int}}$ (10)	$\langle B \rangle_{\text{mag}}$ (11)
V1.....	<i>ab</i>	0.64717	15.96	1.05	16.573	16.617	16.20	1.28	16.907	16.985
V2.....	<i>c</i>	0.37895	16.40	0.49	16.639	16.653	16.59	0.69	16.915	16.941
V3.....	<i>ab</i>	0.59294	16.21	0.69	16.617	16.639	16.37	0.95	16.937	16.982
V4.....	<i>ab</i>	0.66707	15.93	1.05	16.541	16.585	16.03	1.38	16.846	16.932
V5.....	<i>ab</i>	0.71486	16.26	0.60	16.588	16.603	16.52	0.78	16.955	16.983
V6.....	<i>c</i>	0.29219	16.41	0.56	16.700	16.716	16.54	0.70	16.902	16.918
V7.....	<i>c</i>	0.35194	16.33	0.47	16.553	16.566	16.48	0.64	16.760	16.783
V8.....	<i>c</i>	0.36284	16.35	0.58	16.659	16.678	16.52	0.76	16.908	16.940
V9.....	<i>ab</i>	0.74022	16.33	0.50	16.606	16.619	16.58	0.66	16.971	16.994
V10.....	<i>ab</i>	0.77585	16.40	0.24	16.525	16.529	16.74	0.34	16.927	16.933

clusters. The theoretical curve is the expected mean  $dP/dt$  for a metal abundance  $[\text{Fe}/\text{H}] = -2.2$  dex (see Fig. 4 of Lee 1991); it differs little from that for  $[\text{Fe}/\text{H}] = -1.2$  dex. The data are from Stagg & Wehlau (1980), Smith & Sandage (1981), Nemeč et al. (1985), and Wehlau et al. (1999); and the assumed period change rates are as follows:  $0.03 \pm 0.03$  (mean and median) for NGC 7006;  $0.00 \pm 0.03$  for M3, NGC 6934, and M5;  $0.04 \pm 0.03$  for M22 and M15;  $0.11 \pm 0.03$  for  $\omega$  Cen; and  $0.0 \pm 0.02$  for NGC 2257.

The mean period change rate for the RR Lyrae stars in NGC 5053 is  $dP/dt = +0.04 \pm 0.04$  days  $\text{Myr}^{-1}$  (average of the values in col. [11] of Table 7); the median is  $0.045 \pm 0.04$  days  $\text{Myr}^{-1}$ . Both values lie within one standard error of the prediction from Lee's model. With an HB type  $\sim 0.55$  (Lee, Demarque, & Zinn 1994; Sarajedini & Milone 1995; Sohn 2001) NGC 5053 is an example of a very metal poor globular cluster with a "central" distribution of stars along the HB.

## 5. FOURIER DECOMPOSITION OF THE LIGHT CURVES

Over the last 20 yr Fourier decomposition methods have been successfully used (Simon & Lee 1981; Petersen 1986; Stellingwerf & Donohoe 1986) to characterize the observed photometric light curves of RR Lyrae and other types of

variable stars. Simon and his collaborators compared the measured Fourier *coefficients* (i.e., amplitudes and phases) and the *parameters* derived from the coefficients (i.e., amplitude ratios and phase differences) with theoretical light curves based on hydrodynamical models (Simon & Lee 1981; Simon & Clement 1993; Clement & Rowe 2000) and were able to derive such quantities as absolute magnitude ( $M_V$ ), luminosity ( $L$ ), mass ( $M$ ), and metal abundance  $[\text{Fe}/\text{H}]$  for individual stars. In a parallel effort, Kovács and his collaborators (Jurcsik & Kovács 1996; Kovács & Jurcsik 1996; Jurcsik 1998; Kovács 1998; Kovács & Kanbur 1998; Kovács & Walker 2001; Kovács 2002) were able to derive the same physical characteristics by establishing correlations between the Fourier parameters and the physical quantities of field and cluster variables independently derived from Baade-Wesselink and trigonometric parallax studies.

In this section, Fourier coefficients and parameters are derived from the new photometry and the methods and equations from the above two groups are used to derive absolute magnitudes, luminosities, masses, etc., of the RR Lyrae stars in NGC 5053. Owing to the distinctly different light-curve characteristics of first-overtone (RRc) and fundamental-mode (RRab) pulsators, different models and equations were used for the two types of stars. Similar methods have been used by others to derive the physical characteristics of the RR Lyrae

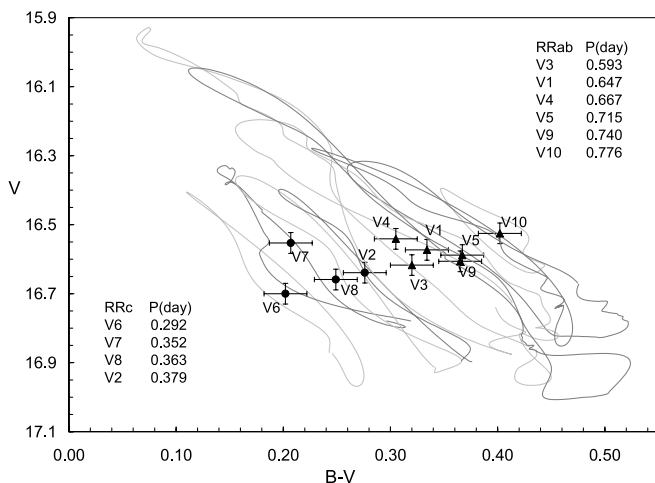


FIG. 3.—Color-magnitude diagram for the 10 RR Lyrae stars in NGC 5053. Loops over the pulsation cycles and intensity-mean colors and magnitudes are shown for each star. The four first-overtone *c*-type RR Lyrae stars are the hottest variables (*filled circles*) and the six *ab*-type RR Lyraes are the coolest (*filled triangles*).

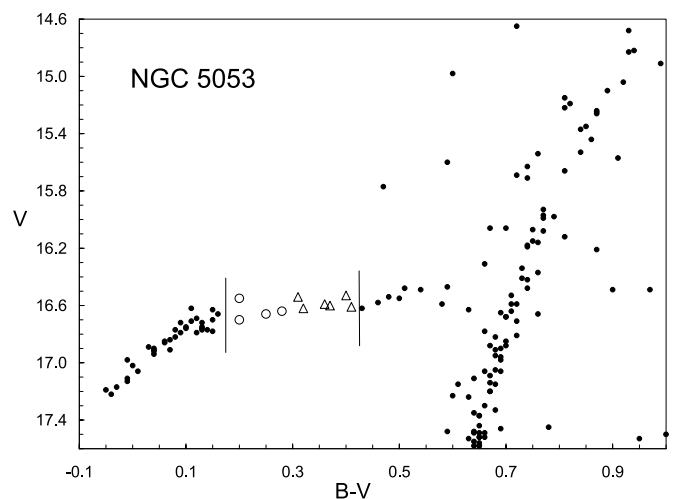


FIG. 4.—Color-magnitude diagram showing the location of the RR Lyrae stars with respect to the nonvariable bright stars in NGC 5053. The mean magnitudes and colors are intensity means.

TABLE 6  
PHASES OF MAXIMUM LIGHT (EPOCHS 1924–2002)

Epoch (1)	HJD (2)	V1 (3)	V2 (4)	V3 (5)	V4 (6)	V5 (7)	V6 (8)	V7 (9)	V8 (10)	V9 (11)	V10 (12)
Assumed Periods and Zero-Point Epochs of Maximum Light											
<i>P</i> (days).....	...	0.6471742	0.378956	0.592943	0.667073	0.714860	0.292188	0.351936	0.362841	0.7402201	0.775851
<i>T</i> <sub>0</sub> .....	...	49452.749	46587.86	46972.694	42708.066	46972.794	48416.660	51609.82	37371.452	37371.407	51608.900
Phases of Maximum Light											
1924 Baade .....	23,830	-0.05 ± 0.05	0.54 ± 0.08	-0.17 ± 0.06	...	...	-3.25 ± 0.20	0.59 ± 0.06	...	...	...
1927 Baade .....	24,990	-0.05 ± 0.05	0.38 ± 0.03	-0.19 ± 0.03	0.26 ± 0.05	-0.20 ± 0.08	-3.20 ± 0.10	0.40 ± 0.05	-1.62 ± 0.10	0.03 ± 0.04	...
1938 Sawyer .....	29,078	0.00 ± 0.10	0.28 ± 0.05	-0.15 ± 0.10	0.18 ± 0.03	-0.20 ± 0.07	-1.80 ± 0.08	-0.55 ± 0.06	-2.12 ± 0.10	0.02 ± 0.05	0.10 ± 0.12
1940 Sawyer .....	29,787	0.00 ± 0.10	0.28 ± 0.05	-0.14 ± 0.10	0.14 ± 0.03	-0.20 ± 0.07	-1.64 ± 0.08	-0.60 ± 0.06	-2.11 ± 0.05	0.00 ± 0.08	0.08 ± 0.07
1941 Sawyer .....	30,170	-0.05 ± 0.12	0.30 ± 0.05	-0.12 ± 0.10	0.12 ± 0.03	-0.17 ± 0.10	-1.59 ± 0.07	-0.57 ± 0.06	-2.10 ± 0.25	0.00 ± 0.10	0.07 ± 0.10
1942 Sawyer .....	30,537	-0.10 ± 0.08	0.30 ± 0.05	-0.15 ± 0.06	0.13 ± 0.03	-0.18 ± 0.07	-1.57 ± 0.08	-0.67 ± 0.08	-2.10 ± 0.10	-0.03 ± 0.04	0.06 ± 0.10
1943 Sawyer .....	30,885	-0.10 ± 0.05	0.25 ± 0.05	-0.16 ± 0.05	0.10 ± 0.03	-0.25 ± 0.05	-1.54 ± 0.14	-0.54 ± 0.07	-2.10 ± 0.10	-0.02 ± 0.05	0.10 ± 0.07
1944 Rosino .....	31,200	-0.05 ± 0.05	0.26 ± 0.07	-0.15 ± 0.06	0.08 ± 0.04	-0.17 ± 0.07	-1.52 ± 0.01	...	-2.11 ± 0.12	-0.04 ± 0.05	0.03 ± 0.08
1944 Sawyer .....	31,259	-0.11 ± 0.03	0.20 ± 0.05	-0.16 ± 0.04	0.10 ± 0.03	-0.25 ± 0.10	-1.48 ± 0.07	-0.58 ± 0.07	-2.12 ± 0.10	-0.04 ± 0.04	0.06 ± 0.08
1946 Rosino .....	31,976	-0.02 ± 0.06	0.26 ± 0.07	-0.19 ± 0.04	0.08 ± 0.04	-0.20 ± 0.07	-1.43 ± 0.10	-0.71 ± 0.07	-2.06 ± 0.10	-0.03 ± 0.05	0.04 ± 0.10
1946 Sawyer .....	31,990	-0.04 ± 0.04	0.21 ± 0.04	-0.13 ± 0.04	0.09 ± 0.03	-0.19 ± 0.05	-1.44 ± 0.05	-0.76 ± 0.07	-2.10 ± 0.05	-0.03 ± 0.04	0.08 ± 0.07
1947 Rosino .....	32,275	-0.04 ± 0.04	0.20 ± 0.09	-0.17 ± 0.03	0.08 ± 0.04	-0.14 ± 0.07	...	...	-2.06 ± 0.07	-0.02 ± 0.05	0.02 ± 0.07
1949 Rosino .....	32,990	-0.05 ± 0.05	0.20 ± 0.09	-0.10 ± 0.07	0.08 ± 0.04	-0.27 ± 0.07	-1.28 ± 0.10	...	-2.08 ± 0.11	-0.03 ± 0.06	0.00 ± 0.07
1961 Mannino .....	37,344	-0.05 ± 0.08	0.20 ± 0.10	-0.13 ± 0.03	0.00 ± 0.04	-0.25 ± 0.07	-0.75 ± 0.10	-1.08 ± 0.10	-1.96 ± 0.04	0.01 ± 0.05	0.04 ± 0.06
1962 Mannino .....	37,790	0.00 ± 0.05	0.22 ± 0.07	-0.13 ± 0.03	-0.03 ± 0.04	-0.20 ± 0.04	-0.68 ± 0.10	-1.08 ± 0.07	-1.94 ± 0.04	0.01 ± 0.05	0.03 ± 0.10
1985 Feb 19–22 .....	46,118	...	...	...	-0.10 ± 0.03	...	...	...	...	...	...
1986 Jun 5–7 .....	46,588	-0.13 ± 0.12	0.08 ± 0.12	...	...	...	...	-0.01 ± 0.04	...	...	...
1987 Apr–Jun .....	46,915	0.05 ± 0.07	0.01 ± 0.07	-0.03 ± 0.04	-0.10 ± 0.10	-0.10 ± 0.07	0.03 ± 0.03	-0.01 ± 0.05	-0.99 ± 0.04	...	-0.03 ± 0.03
1988 Feb–Mar .....	47,220	...	...	...	-0.09 ± 0.03	...	...	...	...	...	0.03 ± 0.04
1991 Jun 8/9 .....	48,417	...	...	-0.01 ± 0.02	-0.11 ± 0.03	...	0.02 ± 0.03	0.03 ± 0.02	-0.73 ± 0.03	...	-0.03 ± 0.07
1994 Mar–May .....	49,450	0.00 ± 0.04	-0.03 ± 0.03	0.00 ± 0.02	-0.12 ± 0.03	-0.09 ± 0.02	0.05 ± 0.03	0.09 ± 0.02	-0.59 ± 0.03	-0.02 ± 0.05	0.03 ± 0.04
1995 Feb–Apr .....	49,800	-0.04 ± 0.04	-0.01 ± 0.04	0.03 ± 0.03	-0.12 ± 0.03	-0.07 ± 0.04	0.09 ± 0.03	0.11 ± 0.02	-0.54 ± 0.03	-0.07 ± 0.07	-0.02 ± 0.03
1999 Apr–Jun .....	51,310	0.06 ± 0.03	-0.06 ± 0.03	0.06 ± 0.03	-0.17 ± 0.05	...	0.04 ± 0.03	1.00 ± 0.01	-0.26 ± 0.07	-0.02 ± 0.05	0.02 ± 0.06
2000 Mar–Jun .....	51,630	-0.01 ± 0.08	-0.06 ± 0.03	0.06 ± 0.02	-0.12 ± 0.03	...	0.02 ± 0.03	1.00 ± 0.01	-0.19 ± 0.02	-0.08 ± 0.05	0.00 ± 0.03
2001 May–Jun .....	52,067	...	-0.11 ± 0.02	0.06 ± 0.02	-0.12 ± 0.02	-0.04 ± 0.02	0.00 ± 0.01	1.00 ± 0.01	-0.11 ± 0.03	...	-0.04 ± 0.02
2002 Feb–May .....	52,322	-0.04 ± 0.05	-0.14 ± 0.03	0.05 ± 0.03	-0.12 ± 0.01	-0.04 ± 0.02	-0.03 ± 0.03	1.02 ± 0.02	-0.07 ± 0.03	0.00 ± 0.05	-0.04 ± 0.02

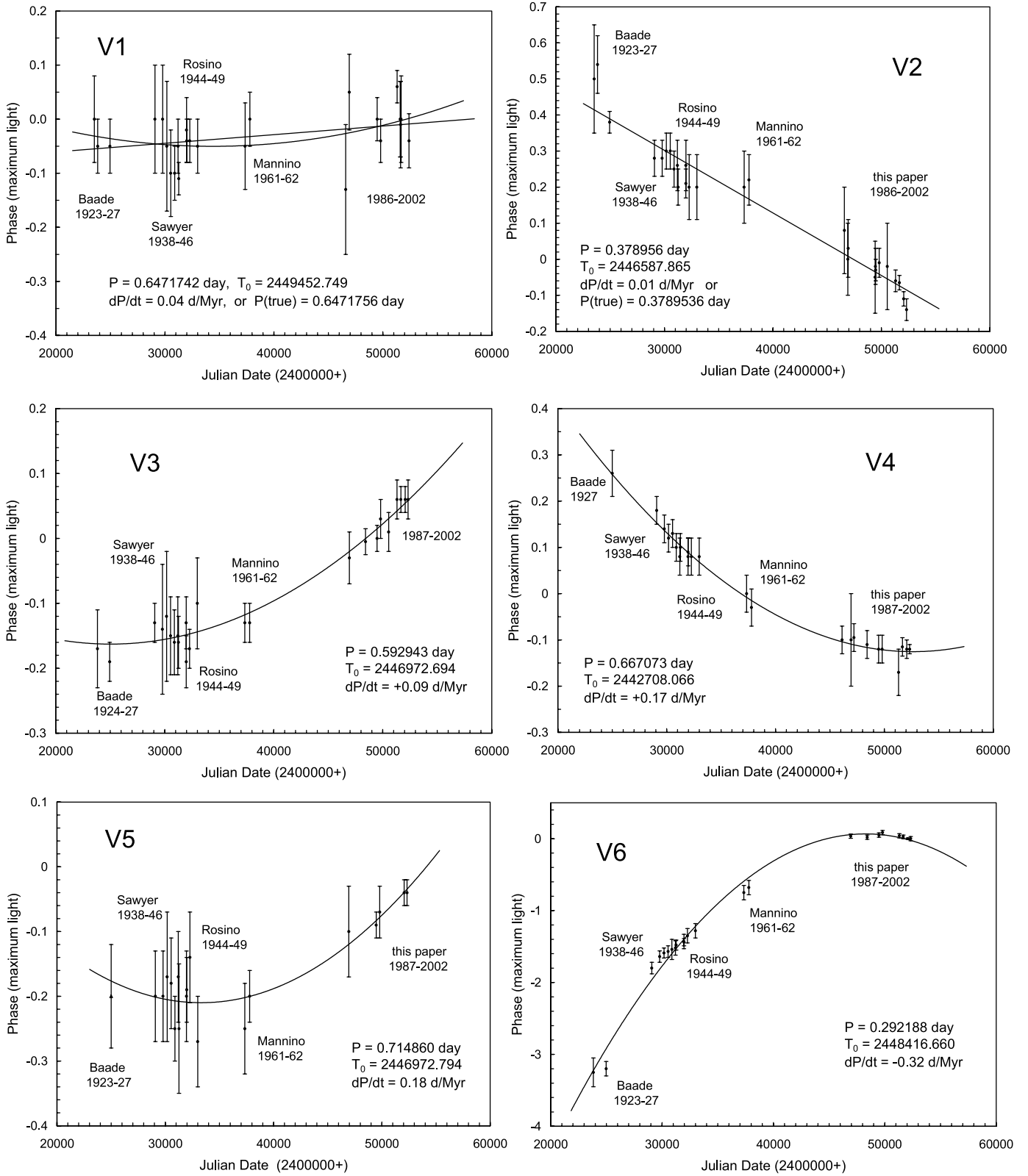


FIG. 5.—(a) Phase-shift diagrams used to derive period change rates ( $dP/dt$ ) for V1–V6. The ordinate is the phase at maximum light derived from light curves that assume the  $P$  noted in the diagram.  $T_0$  is the (arbitrary) epoch of zero phase for the light curves (from which the phases of maximum light were measured). (b) Same as (a), but for V7–V10. Two candidate solutions for V7 are shown.

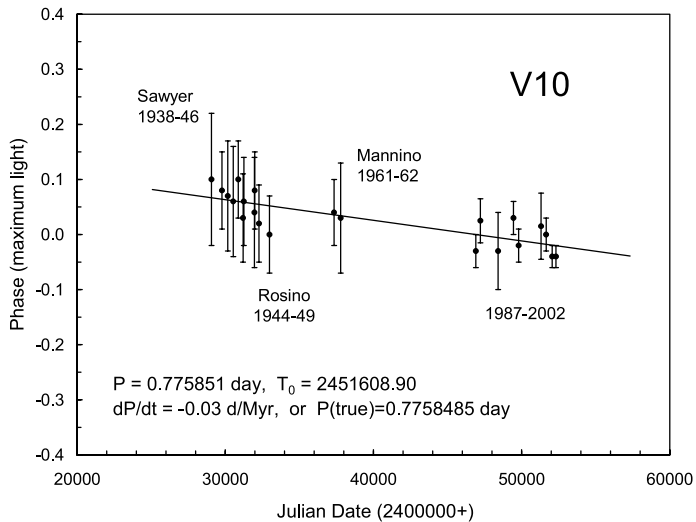
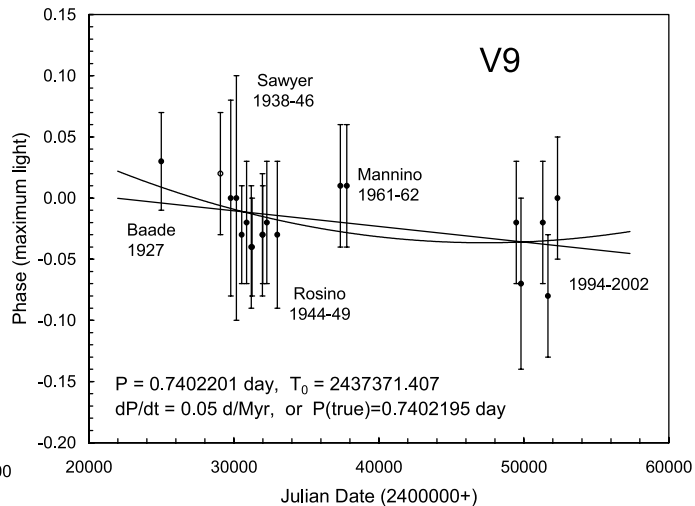
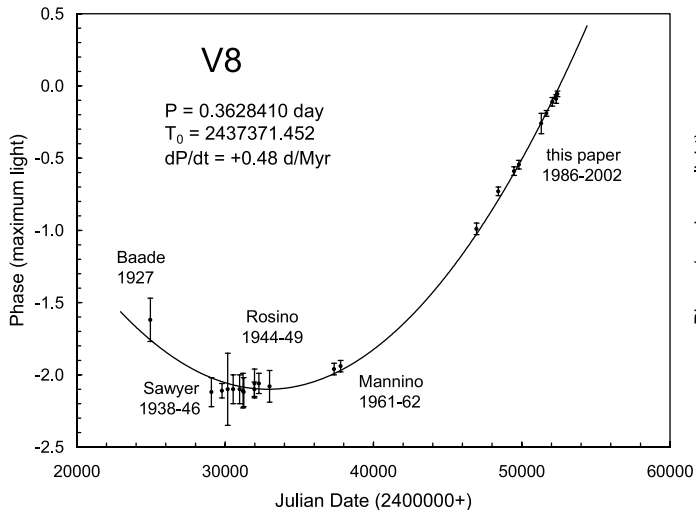
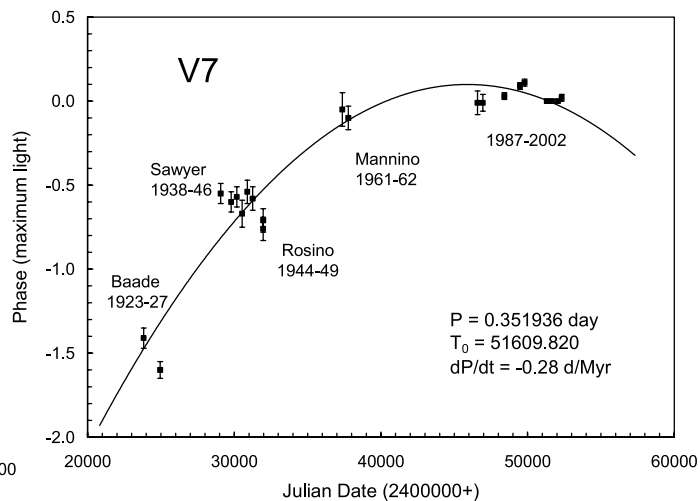
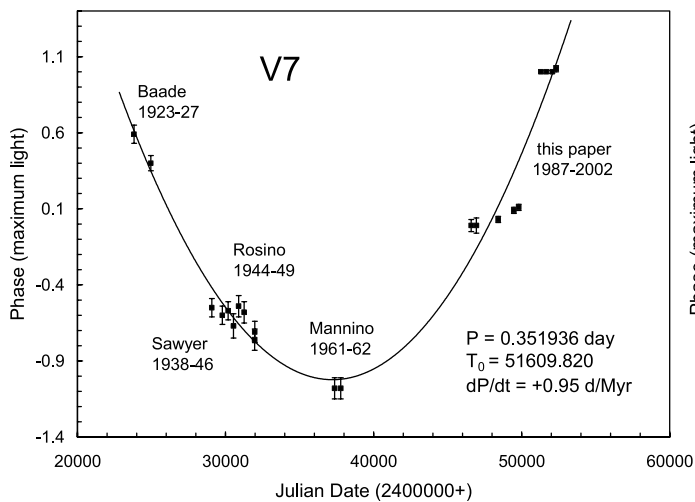


FIG. 5.—Continued

TABLE 7  
QUADRATIC FITS TO PHASE-SHIFT OBSERVATIONS: PERIOD CHANGE RATES

Star (1)	RR Type (2)	Assumed $P$ (days) (3)	$a$ (4)	$b \times 10^5$ (5)	$c \times 10^{10}$ (6)	$\sigma_{\text{rms}}$ (7)	$R^2$ (8)	No. Pts. (9)	Epoch of Assumed $P$ (10)	$dP/dt$ (days Myr $^{-1}$ ) (11)
V1.....	<i>ab</i>	0.6471742	+0.02 ± 0.23	+0.6 ± 1.2	+1.2 ± 1.5	0.042	0.42	22	2,426,028	+0.04 ± 0.05
V2.....	<i>c</i>	0.378956	+0.87 ± 0.23	-2.1 ± 1.2	+0.4 ± 1.5	0.036	0.97	23	2,634,289	+0.01 ± 0.02
V3.....	<i>ab</i>	0.592943	+0.05 ± 0.09	-1.7 ± 0.5	+3.4 ± 0.6	0.015	0.98	23	2,425,717	+0.09 ± 0.02
V4.....	<i>ab</i>	0.667073	+1.29 ± 0.09	-5.4 ± 0.5	+5.2 ± 0.6	0.011	0.99	24	2,452,025	+0.17 ± 0.02
V5.....	<i>ab</i>	0.714860	+0.32 ± 0.19	-3.2 ± 1.0	+4.8 ± 1.2	0.020	0.93	19	2,433,353	+0.18 ± 0.05
V6.....	<i>c</i>	0.292188	-12.13 ± 0.48	+50.0 ± 2.5	-51.3 ± 3.0	0.036	1.00	22	2,448,732	-0.32 ± 0.02
V7.....	<i>c</i>	0.351936	-6.50 ± 0.61	+28.4 ± 3.2	-30.6 ± 4.0	0.056	0.95	21	2,446,443	-0.28 ± 0.04
V8.....	<i>c</i>	0.3628410	+3.11 ± 0.26	-32.4 ± 1.3	+50.3 ± 1.6	0.029	1.00	22	2,432,183	+0.48 ± 0.02
V9.....	<i>ab</i>	0.7402201	+0.21 ± 0.18	-1.1 ± 0.9	+1.2 ± 1.1	0.027	0.19	19	2,444,433	+0.05 ± 0.05
V10.....	<i>ab</i>	0.775851	+0.10 ± 0.26	+0.1 ± 1.3	-0.6 ± 1.6	0.025	0.63	22	2,405,290	-0.03 ± 0.07

stars in other globular clusters (Olech et al. 1999, 2001; Corwin et al. 2003).

### 5.1. Fourier Coefficients

Fourier decomposition coefficients for the RR Lyrae stars in NGC 5053 were computed for both the  $V$  and  $B$  photometry. The observed magnitudes were fitted with a Fourier sine series of the form

$$\text{mag} = A_0 + \sum_{i=1}^N A_i \sin(i\omega t + \phi_i), \quad (1)$$

where  $\omega = 2\pi/P$  is the angular frequency,  $t$  is the time of the observation, and the  $A_i$  and  $\phi_i$  are the Fourier coefficients. The fits were made using two FORTRAN programs kindly supplied by Geza Kovács, one for simple light curves and the other for more complex light curves; the two programs give identical results for simple light curves.

The derived Fourier coefficients  $\phi_i(V)$ ,  $\phi_i(B)$ ,  $A_i(V)$ , and  $A_i(B)$  for the NGC 5053 stars are given in Table 9. The assumed period ( $P$ ), the epoch of maximum light ( $T_0$ ), the subset of the photometric data that was analyzed (important when the period is changing), the Fourier fitted mean magnitude level [ $A_V(0)$ ,  $A_B(0)$ ], the standard deviation of the Fourier fit ( $\sigma_V$ ,  $\sigma_B$ ), and the number of points in the fit ( $N$ ) are recorded in the column header. Depending on the quality of the photometry and the nature of the light variations, the number of terms in the sine series (i.e., the order of the Fourier series) varied from star to star. Usually six to eight terms were used; however, 15 terms were necessary to model the shoulder on the rise to maximum light for V5, and nine terms were needed to model

successfully the structure seen at minimum light for the  $V$  photometry of V4.

In general, the first five Fourier amplitude coefficients fall within the range of observed values for globular cluster stars—see Table 1 of Kovács & Kanbur (1998), which gives the coefficient ranges for 257 RRab stars in many globular clusters and in the Sculptor dwarf galaxy. An exception is the longest period NGC 5053 star, V10 with  $P = 0.775851$  days, which has several amplitudes ( $A_2 = 0.034 \pm 0.001$ ,  $A_3 = 0.013 \pm 0.001$ , and  $A_4 = 0.005 \pm 0.001$ ) that are less than the respective minimum amplitudes obtained by Kovács & Kanbur (1998) (min  $A_2 = 0.06$ ; min  $A_3 = 0.02$ ; and min  $A_4 = 0.01$ ). Possibly the former small values are due to the extremely low metal abundance of NGC 5053.

### 5.2. Fourier Parameters

The Fourier parameters associated with the most significant (lowest order) Fourier coefficients are presented in Table 10 for the RRc stars pulsating in the first-overtone mode, and in Table 11 for the RRab stars pulsating in the fundamental mode. In both tables, the stars are listed in order of increasing pulsation period.

Table 10 contains the estimated amplitude ratios for each filter,  $A_{i1}(V) = A_i(V)/A_1(V)$  and  $A_{i1}(B) = A_i(B)/A_1(B)$ , and the corresponding phase differences,  $\phi_{i1}^s(V, B) = \phi_i(V, B) - i\phi_1(V, B)$ . The  $\phi_{i1}$ -values have been adjusted so that the mean values lie between 0 and  $2\pi$ ; thus, they are comparable to the values given by Jurcsik & Kovács (1996).

Table 11 contains, in addition to the above quantities, the amplitude parameters,  $A_i(V)\text{calc}$  and  $A_i(B)\text{calc}$ ; phase parameters,  $\phi_{i1}^s(V)\text{calc}$  and  $\phi_{i1}^s(B)\text{calc}$ ; and deviation parameters calculated using the equations given in Table 6 of Jurcsik &

TABLE 8  
LINEAR FITS TO PHASE-SHIFT OBSERVATIONS: REVISED (CONSTANT) PERIODS

Star (1)	RR Type (2)	Assumed $P$ (days) (3)	Epoch of Maximum Light (4)	$a$ (5)	$b \times 10^6$ (6)	$\sigma_{\text{rms}}$ (7)	$R^2$ (8)	$P$ , If Constant (days) (9)
V1.....	<i>ab</i>	0.6471742	2,449,452.749	-0.161 ± 0.036	+3.3 ± 0.9	0.041	0.40	0.6471756 (±4)
V2.....	<i>c</i>	0.378956	2,452,050.855	+0.801 ± 0.030	-17.2 ± 0.7	0.035	0.97	0.3789536 (±2)
V3.....	<i>ab</i>	0.592943	2,446,972.694	-0.464 ± 0.024	+9.8 ± 0.5	0.024	0.94	0.5929464 (±2)
V4.....	<i>ab</i>	0.667073	2,442,708.066	+0.462 ± 0.022	-11.3 ± 0.5	0.024	0.96	0.6670679 (±2)
V5.....	<i>ab</i>	0.714860	2,446,972.794	-0.452 ± 0.034	+7.7 ± 0.7	0.028	0.86	0.7148639 (±4)
V9.....	<i>ab</i>	0.7402201	2,437,371.407	+0.021 ± 0.026	-1.1 ± 0.7	0.027	0.13	0.7402195 (±4)
V10.....	<i>ab</i>	0.775851	2,451,608.900	+0.191 ± 0.034	-4.2 ± 0.7	0.024	0.63	0.7758485 (±4)

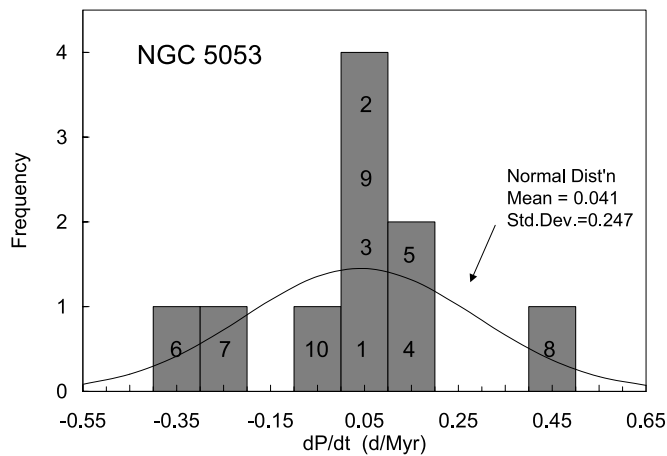


FIG. 6.—Histogram of the period change rates (days  $\text{Myr}^{-1}$ ) for the 10 RR Lyrae stars in NGC 5053. The number in each cell is the variable star number, and the curve is the best-fit normal distribution.

Kovács (1996). The maxima of the individual  $DA$ - and  $D\phi^s$ -values have been underlined for each filter; these correspond to the Jurcsik-Kovács “maximum deviation parameter,”  $D_m$ . Such  $D_m$  values were also computed for the  $V$  data using the newer Kovács & Kanbur (1998) interrelations, with smaller but similar results (see Table 17 below).

## 6. MEAN COLORS AND REDDENING

Mean colors for the individual RR Lyrae stars are useful for estimating effective temperatures and, with reddening-free colors, for estimating the interstellar reddening,  $E_{B-V}$ , of the parent cluster.

### 6.1. Mean $B-V$ Colors

Mean  $B-V$  colors for the NGC 5053 RR Lyrae stars are contained in Table 12. The intensity- and magnitude-averaged colors,  $\langle B \rangle - \langle V \rangle$  in columns (3) and (4) were computed using the mean magnitudes given in Table 5; the uncertainties are typically  $\pm 0.020$  mag. As expected, the magnitude-averaged colors tend to be slightly redder than the intensity-averaged

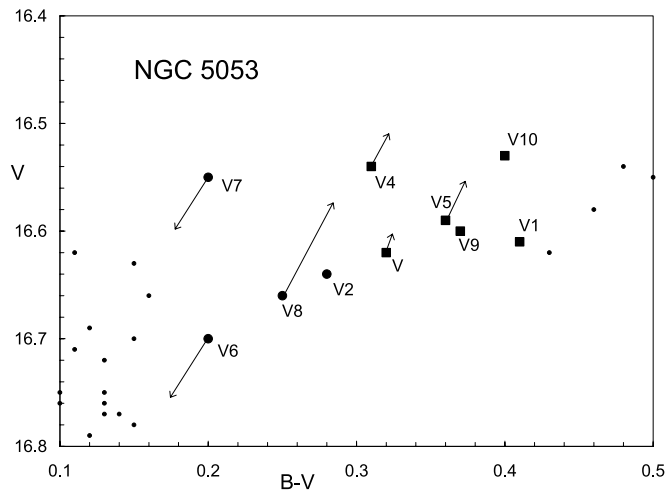


FIG. 7.—Color-magnitude diagram in the region of the instability strip of the HB. The RRab stars are shown as filled squares, and the RRc stars are plotted as filled circles. The vectors represent the derived period change rates, with the largest rates occurring for the shortest period stars. The smaller solid dots to the left and right are nonvariable HB stars from the study by Sarajedini & Milone (1995).

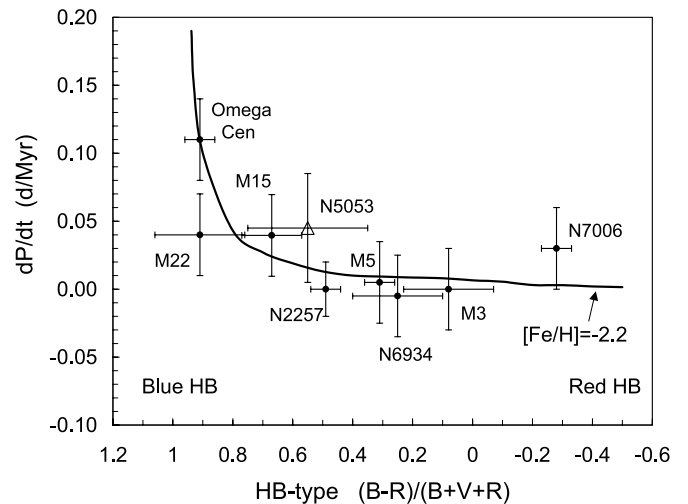


FIG. 8.—HB type vs. period change rate diagram for selected well-studied globular clusters. For each cluster, the mean (or median) period change rate is plotted. The theoretical curve is from Lee (1991).

colors (Preston 1961). The shortest period RR Lyrae star, V6 with  $\langle B \rangle_{\text{int}} - \langle V \rangle_{\text{int}} = 0.20 \pm 0.02$ , is the bluest star and, therefore, probably lies close to the first-overtone blue edge (HBE) of the instability strip for stars with  $[\text{Fe}/\text{H}] = -2.3$  dex. Similarly, the longest period and reddest RR Lyrae variable, V10, with  $\langle B \rangle_{\text{int}} - \langle V \rangle_{\text{int}} = 0.40 \pm 0.02$ , probably lies close to the fundamental-mode red edge (FRE, see Fig. 9).

The magnitude-averaged colors  $(B-V)_{\text{mag}}$  in column (5) of Table 12 were computed using the colors in column (3) modified by the Sandage (1990) prescription for an “equivalent static star,” that is to say,

$$(B-V)_{\text{mag}} = \langle B \rangle_{\text{int}} - \langle V \rangle_{\text{int}} + \Delta C(A_B). \quad (2)$$

The agreement with the magnitude-averaged colors in column (4) is good.

The magnitude-averaged colors for the RRab stars (in col. [6] of Table 12) were derived from the data given in Carney, Storm, & Jones (1992), as summarized by Carretta, Gratton, & Clementini (2000):

$$(B-V)_{\text{mag}} = 0.672(\langle B \rangle_{\text{int}} - \langle V \rangle_{\text{int}}) + 0.134. \quad (3)$$

The colors agree well with the magnitude-averaged colors in column (4) and with the “S90” colors in column (5).

The magnitude-averaged colors for the RRc stars (top half of col. [6]) were found to agree with the magnitude-averaged colors in column (4) if a small offset was applied to the intensity-averaged magnitudes, i.e.,

$$(B-V)_{\text{mag}} = (\langle B \rangle - \langle V \rangle)_{\text{int}} + 0.007. \quad (4)$$

‘Dereddened’ colors for the RRc stars were computed with the Simon & Clement (1993) equation for  $T_{\text{eff}}$ , transformed to  $(B-V)_0$ , using a semiempirical color-temperature transformation derived from Vandenberg (2000) and Vandenberg & Clem (2003), and are given in the upper half of column (7). The RRab estimates (lower half of col. [7]) are the average of two Fourier-based values:

$$(B-V)_0 = 0.308 + 0.163P - 0.187A_1 \quad (5)$$



TABLE 9—Continued

C. Amplitudes and Phases Derived from the *B* Photometry

<i>i</i>	V1		V2		V3		V4		V5		V6		V7		V8		V9		V10	
	<i>A</i> ( <i>i</i> )	$\phi$ ( <i>i</i> )	<i>A</i> ( <i>i</i> )	$\phi$ ( <i>i</i> )	<i>A</i> ( <i>i</i> )	$\phi$ ( <i>i</i> )	<i>A</i> ( <i>i</i> )	$\phi$ ( <i>i</i> )	<i>A</i> ( <i>i</i> )	$\phi$ ( <i>i</i> )	<i>A</i> ( <i>i</i> )	$\phi$ ( <i>i</i> )	<i>A</i> ( <i>i</i> )	$\phi$ ( <i>i</i> )	<i>A</i> ( <i>i</i> )	$\phi$ ( <i>i</i> )	<i>A</i> ( <i>i</i> )	$\phi$ ( <i>i</i> )	<i>A</i> ( <i>i</i> )	$\phi$ ( <i>i</i> )
1.....	0.506	4.42	0.328	4.30	0.379	3.77	0.492	4.76	0.302	4.08	0.327	4.21	0.313	4.42	0.366	4.42	0.267	4.16	0.149	4.35
	±0.024	0.07	0.004	0.01	0.006	0.02	0.005	0.01	0.007	0.02	0.004	0.01	0.003	0.01	0.004	0.01	0.012	0.05	0.003	0.02
2.....	0.212	4.86	0.067	5.52	0.168	3.44	0.236	5.44	0.132	4.31	0.099	4.80	0.045	5.87	0.067	5.36	0.118	4.36	0.049	4.93
	±0.021	0.16	0.004	0.06	0.006	0.03	0.006	0.03	0.006	0.05	0.003	0.03	0.004	0.08	0.004	0.06	0.011	0.09	0.002	0.05
3.....	0.150	5.73	0.025	6.18	0.100	3.53	0.163	0.29	0.085	4.92	0.030	5.73	0.020	1.02	0.028	5.79	0.058	4.83	0.013	5.93
	±0.031	0.24	0.003	0.14	0.006	0.06	0.006	0.03	0.006	0.07	0.004	0.13	0.004	0.18	0.004	0.14	0.009	0.18	0.003	0.19
4.....	0.088	0.32	0.013	2.34	0.048	3.77	0.112	1.47	0.041	5.58	0.013	5.99	0.016	2.38	0.012	2.50	0.028	5.74	0.008	0.50
	±0.057	0.30	0.004	0.32	0.007	0.11	0.005	0.04	0.007	0.16	0.004	0.28	0.004	0.23	0.004	0.34	0.012	0.40	0.003	0.31
5.....	0.053	1.24	0.003	3.51	0.021	4.00	0.066	2.57	0.018	6.27	0.017	1.07	0.009	3.15	0.010	3.28	0.018	6.18	0.004	4.23
	±0.055	0.83	0.003	3.12	0.006	0.36	0.006	0.08	0.005	0.40	0.004	0.22	0.003	0.41	0.003	0.34	0.010	0.69	0.003	0.59
6.....	0.034	2.21	0.008	4.09	0.008	4.17	0.039	3.62	0.008	0.78	0.010	1.12	0.007	3.91	0.006	4.02	0.012	1.69	0.005	4.06
	±0.049	3.03	0.004	0.49	0.006	0.41	0.006	0.17	0.005	0.71	0.004	0.39	0.004	0.42	0.003	0.39	0.010	1.17	0.003	0.48
7.....	0.023	3.21	0.006	5.38	0.003	4.28	0.022	4.66	0.004	1.80	0.002	0.79	0.001	3.87	0.006	3.89	...	...	...	...
	±0.030	3.14	0.004	0.58	0.005	2.75	0.005	0.16	0.006	0.87	0.003	3.12	0.003	3.08	0.004	0.98	...	...	...	...
8.....	0.017	4.20	0.010	6.22	...	...	0.013	5.73	...	...	...	...	0.004	3.62	0.002	3.96	...	...	...	...
	±0.021	3.12	0.003	0.39	...	...	0.006	0.27	...	...	...	...	0.004	0.46	0.004	0.77	...	...	...	...
9.....	0.012	5.11	...	...	...	...	...	...	...	...	...	...	0.002	5.11	...	...	...	...	...	...
	±0.013	1.29	...	...	...	...	...	...	...	...	...	...	0.003	1.40	...	...	...	...	...	...

TABLE 10  
FOURIER PARAMETERS FOR RR<sub>C</sub> STARS IN NGC 5053

Parameter	$i = 2$	$i = 3$	$i = 4$	$i = 5$	$i = 6$
V6 ( $P = 0.292188$ days)					
$A_{i1}(V)$ .....	$0.300 \pm 0.013$	$0.067 \pm 0.011$	$0.029 \pm 0.009$	$0.034 \pm 0.009$	$0.020 \pm 0.009$
$A_{i1}(B)$ .....	$0.303 \pm 0.013$	$0.090 \pm 0.013$	$0.039 \pm 0.013$	$0.053 \pm 0.013$	$0.029 \pm 0.013$
$\phi_{i1}^s(V)$ .....	$2.66 \pm 0.06$	$5.66 \pm 0.20$	$1.84 \pm 0.41$	$5.48 \pm 0.35$	$1.29 \pm 0.66$
$\phi_{i1}^s(B)$ .....	$2.66 \pm 0.06$	$5.67 \pm 0.16$	$1.72 \pm 0.32$	$5.16 \pm 0.27$	$1.00 \pm 0.45$
V7 ( $P = 0.351936$ days)					
$A_{i1}(V)$ .....	$0.137 \pm 0.010$	$0.060 \pm 0.009$	$0.051 \pm 0.009$	$0.043 \pm 0.009$	$0.017 \pm 0.009$
$A_{i1}(B)$ .....	$0.144 \pm 0.010$	$0.064 \pm 0.010$	$0.051 \pm 0.010$	$0.029 \pm 0.010$	$0.022 \pm 0.010$
$\phi_{i1}^s(V)$ .....	$3.27 \pm 0.10$	$6.47 \pm 0.20$	$3.37 \pm 0.22$	$6.51 \pm 0.25$	$2.51 \pm 0.52$
$\phi_{i1}^s(B)$ .....	$3.31 \pm 0.10$	$6.60 \pm 0.20$	$3.54 \pm 0.20$	$6.18 \pm 0.20$	$2.51 \pm 0.20$
V8 ( $P = 0.3628468$ days)					
$A_{i1}(V)$ .....	$0.200 \pm 0.011$	$0.075 \pm 0.008$	$0.019 \pm 0.008$	$0.033 \pm 0.007$	$0.021 \pm 0.008$
$A_{i1}(B)$ .....	$0.183 \pm 0.010$	$0.077 \pm 0.010$	$0.033 \pm 0.010$	$0.027 \pm 0.010$	$0.016 \pm 0.010$
$\phi_{i1}^s(V)$ .....	$2.80 \pm 0.07$	$5.38 \pm 0.13$	$3.11 \pm 0.45$	$7.88 \pm 0.27$	$3.61 \pm 0.45$
$\phi_{i1}^s(B)$ .....	$2.81 \pm 0.10$	$5.10 \pm 0.15$	$3.68 \pm 0.50$	$6.33 \pm 0.40$	$2.65 \pm 0.50$
V2 ( $P = 0.3789535$ days)					
$A_{i1}(V)$ .....	$0.186 \pm 0.009$	$0.088 \pm 0.006$	$0.020 \pm 0.008$	$0.003 \pm 0.005$	$0.023 \pm 0.007$
$A_{i1}(B)$ .....	$0.206 \pm 0.015$	$0.076 \pm 0.011$	$0.039 \pm 0.013$	$0.009 \pm 0.010$	$0.025 \pm 0.013$
$\phi_{i1}^s(V)$ .....	$3.12 \pm 0.06$	$5.96 \pm 0.08$	$3.93 \pm 0.38$	$5.54 \pm 3.17$	$4.45 \pm 0.34$
$\phi_{i1}^s(B)$ .....	$3.20 \pm 0.10$	$5.83 \pm 0.18$	$3.97 \pm 0.37$	$7.11 \pm 3.18$	$3.39 \pm 0.56$

(Jurcsik 1998, eq. [3]), and

$$(B-V)_0 = 0.460 + 0.189 \log P - 0.313A_1 + 0.293A_3 \quad (6)$$

(Kovács 2002, eq. [3]), which give almost identical results.

### 6.2. $E_{B-V}$ Reddening

With its location  $\sim 16$  kpc above the plane of the Galaxy ( $l = 335^\circ.6$ ,  $b = 78^\circ.9$ ), the reddening of NGC 5053 is expected to be small, although the exact value remains uncertain. Sandage et al. (1977) derived  $E_{B-V} = 0.01 \pm 0.02$ . More recently, Fahlman, Richer, & Nemeč (1991), Sarajedini & Milone (1995), and Sohn (2001) derived the value 0.06. An average of these, 0.04, is listed in the most recent on-line catalog of Harris (1996). Comparing the observed  $B-V$  colors and the Fourier-based dereddened colors provides an independent and direct estimate of the cluster reddening. Assuming that extinction is the same across the face of the cluster, the cluster mean  $E_{B-V}$  is here obtained first by averaging the reddening estimates for the individual RR Lyrae stars (see Kovács 2002).

Individual reddening values for the RR<sub>C</sub> stars were calculated by subtracting the “(SC93, VdB)” values for  $(B-V)_0$  (col. [7]) from the observed magnitude-averaged colors (col. [4]); these are given in column (8) of Table 12. Depending on whether or not the outliers are included in the average, the resulting means are  $E_{B-V} = 0.031 \pm 0.012$  if V2 and V8 are included, and  $0.013 \pm 0.003$  if they are excluded, with the latter being preferred.

The reddenings of the individual RR<sub>ab</sub> stars were calculated in two ways: (1) by subtracting the “unreddened” colors, represented by the column (7) ⟨J98, K02⟩ Fourier values for  $(B-V)_0$ , from the observed column (4) “reddened” magnitude-

averaged colors; and (2) by subtracting the column (7) ⟨J98, K02⟩ colors from the observed column (6) “reddened” colors represented by the “CGC(int)” intensity-averaged values. In both cases (bottom halves of cols. [8] and [9]), the mean reddening is negligible, in agreement with the (preferred) RR<sub>C</sub> result. Thus, the observed RR Lyrae colors are more consistent with  $E_{B-V} = 0.00$  than 0.06 mag.

Another estimate of  $E_{B-V}$  was made using the Schlegel, Finkbeiner, & Davis (1998) maps (hereafter SFD maps) derived from *IRAS* and DIRBE data. Assuming the above galactic coordinates a value of  $0.018 \pm 0.003$  was derived for NGC 5053, again consistent with the RR Lyrae and Sandage et al. (1977) estimates.

## 7. SURFACE GRAVITIES AND EFFECTIVE TEMPERATURES

Surface gravity and  $T_{\text{eff}}$  estimates for the RR Lyrae stars in NGC 5053 are summarized in Table 13. The  $\log g$  values were computed using equations from Fernie (1995), Jurcsik (1998), and Kovács & Walker (1999). The Jurcsik and Kovács & Walker gravities are similar, and both estimates are slightly smaller than the Fernie values—see the scatter among these and various other  $\log g$  values in Figure 3 of Vandenberg & Clem (2003).

The  $\log T_{\text{eff}}$  values in column (6) were computed using the  $\langle B \rangle_{\text{mag}} - \langle V \rangle_{\text{mag}}$  colors given in column (4) of Table 12, transformed to  $T_{\text{eff}}$  through a semiempirical color-temperature relation derived from Table 6 of Vandenberg (2000):  $y = -6.4502x^5 + 15.93x^4 + 3.5881x^2 - 0.7877x + 3.9456$ , where  $x = \langle B \rangle_{\text{mag}} - \langle V \rangle_{\text{mag}}$ ,  $y = \log T_{\text{eff}}$ , and the relation assumes  $[\text{Fe}/\text{H}] = -2.31$  and  $[\alpha/\text{Fe}] = 0.30$ . The resulting temperatures are on the same scale for the RR<sub>C</sub> and RR<sub>ab</sub> stars, and therefore one expects the relative ordering to be correct. Temperatures computed in the same way, but assuming

TABLE 11  
FOURIER PARAMETERS FOR RRab STARS IN NGC 5053

Parameter	$i = 1$	$i = 2$	$i = 3$	$i = 4$	$i = 5$	$i = 6$
V3 ( $P = 0.592943$ days)						
$A_i(V)$ .....	$0.274 \pm 0.003$	$0.110 \pm 0.003$	$0.074 \pm 0.003$	$0.035 \pm 0.003$	$0.010 \pm 0.003$	$0.008 \pm 0.003$
$A_i(V)$ calc.....	$0.267 \pm 0.009$	$0.111 \pm 0.007$	$0.073 \pm 0.002$	$0.035 \pm 0.003$	$0.017 \pm 0.003$	...
$A_i(B)$ .....	$0.379 \pm 0.006$	$0.168 \pm 0.006$	$0.100 \pm 0.006$	$0.048 \pm 0.007$	$0.021 \pm 0.006$	$0.008 \pm 0.006$
$A_i(B)$ calc.....	$0.351 \pm 0.016$	$0.176 \pm 0.012$	$0.099 \pm 0.006$	$0.052 \pm 0.005$	$0.022 \pm 0.005$	...
$A_{i1}(V)$ .....	$1.00 \pm 0.00$	$0.40 \pm 0.02$	$0.27 \pm 0.01$	$0.13 \pm 0.01$	$0.04 \pm 0.01$	$0.03 \pm 0.01$
$A_{i1}(B)$ .....	$1.00 \pm 0.00$	$0.44 \pm 0.02$	$0.26 \pm 0.02$	$0.13 \pm 0.02$	$0.06 \pm 0.02$	$0.02 \pm 0.02$
$\phi_{i1}^s(V)$ .....	...	$2.33 \pm 0.03$	$4.98 \pm 0.05$	$1.72 \pm 0.09$	$4.19 \pm 0.25$	$0.71 \pm 0.47$
$\phi_{i1}^s(V)$ calc.....	...	$2.41 \pm 0.02$	$5.07 \pm 0.04$	$1.48 \pm 0.17$	$4.32 \pm 0.18$	...
$\phi_{i1}^s(B)$ .....	...	$2.17 \pm 0.05$	$4.78 \pm 0.08$	$1.24 \pm 0.14$	$3.98 \pm 0.37$	$0.38 \pm 0.43$
$\phi_{i1}^s(B)$ calc.....	...	$2.26 \pm 0.05$	$4.78 \pm 0.06$	$1.31 \pm 0.24$	$3.93 \pm 0.19$	...
$DA_i(V)$ .....	$0.70 \pm 0.01$	$0.15 \pm 0.01$	$0.16 \pm 0.01$	$0.05 \pm 0.01$	$3.49 \pm 0.01$	...
$D\phi_{i1}^s(V)$ .....	...	$2.08 \pm 0.04$	$1.97 \pm 0.06$	$5.31 \pm 0.19$	$2.65 \pm 0.31$	...
$DA_i(B)$ .....	$2.73 \pm 0.02$	$0.96 \pm 0.01$	$0.20 \pm 0.01$	$0.92 \pm 0.01$	$0.51 \pm 0.01$	...
$D\phi_{i1}^s(B)$ .....	...	$2.27 \pm 0.07$	$0.13 \pm 0.10$	$1.68 \pm 0.28$	$0.94 \pm 0.42$	...
V1 ( $P = 0.6471742$ days)						
$A_i(V)$ .....	$0.365 \pm 0.003$	$0.162 \pm 0.003$	$0.128 \pm 0.003$	$0.080 \pm 0.003$	$0.062 \pm 0.003$	$0.037 \pm 0.003$
$A_i(V)$ calc.....	$0.350 \pm 0.011$	$0.176 \pm 0.008$	$0.124 \pm 0.002$	$0.089 \pm 0.003$	$0.054 \pm 0.003$	...
$A_i(B)$ .....	$0.506 \pm 0.024$	$0.212 \pm 0.021$	$0.150 \pm 0.031$	$0.088 \pm 0.057$	$0.053 \pm 0.055$	$0.034 \pm 0.049$
$A_i(B)$ calc.....	$0.405 \pm 0.089$	$0.281 \pm 0.068$	$0.150 \pm 0.047$	$0.091 \pm 0.038$	$0.055 \pm 0.040$	...
$A_{i1}(V)$ .....	$1.00 \pm 0.00$	$0.44 \pm 0.01$	$0.35 \pm 0.01$	$0.22 \pm 0.01$	$0.17 \pm 0.01$	$0.10 \pm 0.01$
$A_{i1}(B)$ .....	$1.00 \pm 0.00$	$0.42 \pm 0.05$	$0.30 \pm 0.06$	$0.17 \pm 0.11$	$0.10 \pm 0.11$	$0.07 \pm 0.10$
$\phi_{i1}^s(V)$ .....	...	$2.40 \pm 0.03$	$5.06 \pm 0.04$	$1.48 \pm 0.05$	$4.27 \pm 0.07$	$0.76 \pm 0.10$
$\phi_{i1}^s(V)$ calc.....	...	$2.42 \pm 0.02$	$4.99 \pm 0.03$	$1.53 \pm 0.05$	$4.22 \pm 0.06$	...
$\phi_{i1}^s(B)$ .....	...	$2.30 \pm 0.21$	$5.04 \pm 0.31$	$1.49 \pm 0.40$	$4.27 \pm 0.90$	$0.83 \pm 3.06$
$\phi_{i1}^s(B)$ calc.....	...	$2.58 \pm 0.18$	$4.80 \pm 0.21$	$1.54 \pm 0.75$	$4.32 \pm 1.26$	...
$DA_i(V)$ .....	$1.53 \pm 0.01$	$1.80 \pm 0.01$	$0.82 \pm 0.01$	$2.24 \pm 0.01$	$4.18 \pm 0.01$	...
$D\phi_{i1}^s(V)$ .....	...	$0.60 \pm 0.04$	$1.47 \pm 0.05$	$1.14 \pm 0.07$	$1.10 \pm 0.09$	...
$DA_i(B)$ .....	$9.97 \pm 0.07$	$8.41 \pm 0.05$	$0.02 \pm 0.06$	$0.84 \pm 0.07$	$1.05 \pm 0.07$	...
$D\phi_{i1}^s(B)$ .....	...	$6.85 \pm 0.28$	$5.17 \pm 0.37$	$1.17 \pm 0.85$	$0.91 \pm 1.54$	...
V4 ( $P = 0.667073$ days)						
$A_i(V)$ .....	$0.348 \pm 0.003$	$0.175 \pm 0.003$	$0.124 \pm 0.003$	$0.084 \pm 0.003$	$0.051 \pm 0.003$	$0.031 \pm 0.003$
$A_i(V)$ calc.....	$0.355 \pm 0.008$	$0.170 \pm 0.006$	$0.124 \pm 0.002$	$0.080 \pm 0.003$	$0.052 \pm 0.003$	...
$A_i(B)$ .....	$0.492 \pm 0.024$	$0.236 \pm 0.021$	$0.163 \pm 0.031$	$0.112 \pm 0.057$	$0.066 \pm 0.055$	$0.039 \pm 0.049$
$A_i(B)$ calc.....	$0.452 \pm 0.063$	$0.260 \pm 0.047$	$0.168 \pm 0.047$	$0.105 \pm 0.038$	$0.068 \pm 0.040$	...
$A_{i1}(V)$ .....	$1.00 \pm 0.00$	$0.50 \pm 0.01$	$0.36 \pm 0.01$	$0.24 \pm 0.01$	$0.15 \pm 0.01$	$0.09 \pm 0.01$
$A_{i1}(B)$ .....	$1.00 \pm 0.00$	$0.48 \pm 0.01$	$0.33 \pm 0.01$	$0.23 \pm 0.01$	$0.13 \pm 0.01$	$0.08 \pm 0.01$
$\phi_{i1}^s(V)$ .....	...	$2.34 \pm 0.03$	$5.05 \pm 0.04$	$1.53 \pm 0.05$	$4.25 \pm 0.07$	$0.66 \pm 0.10$
$\phi_{i1}^s(V)$ calc.....	...	$2.36 \pm 0.02$	$5.06 \pm 0.02$	$1.49 \pm 0.05$	$4.29 \pm 0.05$	...
$\phi_{i1}^s(B)$ .....	...	$2.20 \pm 0.03$	$4.85 \pm 0.04$	$1.27 \pm 0.05$	$3.89 \pm 0.09$	$0.17 \pm 0.17$
$\phi_{i1}^s(B)$ calc.....	...	$2.35 \pm 0.03$	$4.78 \pm 0.03$	$1.21 \pm 0.07$	$4.04 \pm 0.09$	...
$DA_i(V)$ .....	$0.63 \pm 0.01$	$0.62 \pm 0.01$	$0.06 \pm 0.01$	$0.88 \pm 0.01$	$0.11 \pm 0.01$	...
$D\phi_{i1}^s(V)$ .....	...	$0.43 \pm 0.04$	$0.24 \pm 0.04$	$0.84 \pm 0.07$	$0.79 \pm 0.09$	...
$DA_i(B)$ .....	$3.94 \pm 0.06$	$2.85 \pm 0.04$	$0.89 \pm 0.01$	$1.70 \pm 0.01$	$0.54 \pm 0.01$	...
$D\phi_{i1}^s(B)$ .....	...	$3.63 \pm 0.04$	$1.45 \pm 0.05$	$1.37 \pm 0.09$	$3.12 \pm 0.13$	...
V5 ( $P = 0.714869$ days)						
$A_i(V)$ .....	$0.214 \pm 0.004$	$0.096 \pm 0.003$	$0.073 \pm 0.003$	$0.037 \pm 0.004$	$0.015 \pm 0.004$	$0.006 \pm 0.003$
$A_i(V)$ calc.....	$0.212 \pm 0.014$	$0.102 \pm 0.011$	$0.066 \pm 0.001$	$0.038 \pm 0.003$	$0.016 \pm 0.003$	...
$A_i(B)$ .....	$0.302 \pm 0.007$	$0.132 \pm 0.006$	$0.085 \pm 0.006$	$0.041 \pm 0.007$	$0.018 \pm 0.005$	$0.008 \pm 0.005$
$A_i(B)$ calc.....	$0.269 \pm 0.019$	$0.153 \pm 0.014$	$0.082 \pm 0.006$	$0.044 \pm 0.004$	$0.019 \pm 0.004$	...
$A_{i1}(V)$ .....	$1.00 \pm 0.00$	$0.45 \pm 0.02$	$0.34 \pm 0.02$	$0.17 \pm 0.02$	$0.07 \pm 0.02$	$0.03 \pm 0.02$
$A_{i1}(B)$ .....	$1.00 \pm 0.00$	$0.44 \pm 0.02$	$0.28 \pm 0.02$	$0.14 \pm 0.02$	$0.06 \pm 0.02$	$0.03 \pm 0.02$
$\phi_{i1}^s(V)$ .....	...	$2.50 \pm 0.06$	$5.39 \pm 0.07$	$2.17 \pm 0.13$	$5.64 \pm 0.31$	$2.78 \pm 0.81$
$\phi_{i1}^s(V)$ calc.....	...	$2.60 \pm 0.05$	$5.39 \pm 0.06$	$2.33 \pm 0.22$	$5.42 \pm 0.31$	...
$\phi_{i1}^s(B)$ .....	...	$2.44 \pm 0.07$	$5.26 \pm 0.09$	$1.84 \pm 0.18$	$4.74 \pm 0.41$	$1.46 \pm 0.72$
$\phi_{i1}^s(B)$ calc.....	...	$2.55 \pm 0.07$	$5.17 \pm 0.07$	$1.89 \pm 0.28$	$4.71 \pm 0.30$	...
$DA_i(V)$ .....	$0.19 \pm 0.01$	$0.78 \pm 0.01$	$1.31 \pm 0.01$	$0.20 \pm 0.01$	$0.70 \pm 0.01$	...
$D\phi_{i1}^s(V)$ .....	...	$2.59 \pm 0.08$	$0.05 \pm 0.09$	$3.65 \pm 0.26$	$4.40 \pm 0.44$	...
$DA_i(B)$ .....	$3.24 \pm 0.02$	$2.54 \pm 0.02$	$0.55 \pm 0.01$	$0.80 \pm 0.01$	$0.65 \pm 0.01$	...
$D\phi_{i1}^s(B)$ .....	...	$2.70 \pm 0.09$	$1.77 \pm 0.12$	$1.13 \pm 0.33$	$0.54 \pm 0.51$	...

TABLE 11—Continued

Parameter	$i = 1$	$i = 2$	$i = 3$	$i = 4$	$i = 5$	$i = 6$
V9 ( $P = 0.7402201$ days)						
$A_i(V)$ .....	$0.210 \pm 0.003$	$0.093 \pm 0.002$	$0.038 \pm 0.002$	$0.014 \pm 0.003$	$0.009 \pm 0.002$	$0.004 \pm 0.003$
$A_i(V)$ calc .....	$0.200 \pm 0.014$	$0.092 \pm 0.011$	$0.047 \pm 0.001$	$0.021 \pm 0.002$	$0.006 \pm 0.002$	...
$A_i(B)$ .....	$0.265 \pm 0.012$	$0.116 \pm 0.012$	$0.059 \pm 0.009$	$0.031 \pm 0.012$	$0.018 \pm 0.010$	$0.012 \pm 0.001$
$A_i(B)$ calc .....	$0.276 \pm 0.043$	$0.096 \pm 0.033$	$0.069 \pm 0.010$	$0.035 \pm 0.007$	$0.018 \pm 0.008$	...
$A_{i1}(V)$ .....	$1.00 \pm 0.00$	$0.44 \pm 0.01$	$0.18 \pm 0.01$	$0.07 \pm 0.01$	$0.04 \pm 0.01$	$0.02 \pm 0.01$
$A_{i1}(B)$ .....	$1.00 \pm 0.00$	$0.44 \pm 0.05$	$0.22 \pm 0.04$	$0.12 \pm 0.05$	$0.07 \pm 0.04$	$0.05 \pm 0.04$
$\phi_{i1}^s(V)$ .....	...	$2.64 \pm 0.04$	$5.45 \pm 0.08$	$2.21 \pm 0.18$	$5.14 \pm 0.28$	$2.01 \pm 0.76$
$\phi_{i1}^s(V)$ calc .....	...	$2.63 \pm 0.06$	$5.48 \pm 0.07$	$2.15 \pm 0.20$	$5.05 \pm 0.30$	...
$\phi_{i1}^s(B)$ .....	...	$2.32 \pm 0.14$	$4.90 \pm 0.23$	$1.55 \pm 0.43$	$4.36 \pm 0.77$	$1.80 \pm 1.20$
$\phi_{i1}^s(B)$ calc .....	...	$2.30 \pm 0.15$	$5.05 \pm 0.17$	$1.39 \pm 0.52$	$4.53 \pm 0.54$	...
$DA_i(V)$ .....	$0.99 \pm 0.01$	$0.17 \pm 0.01$	$1.79 \pm 0.01$	$1.58 \pm 0.01$	$1.39 \pm 0.01$	...
$D\phi_{i1}^s(V)$ .....	...	$0.14 \pm 0.07$	$0.65 \pm 0.10$	$1.35 \pm 0.27$	<u>1.93</u> $\pm 0.41$	...
$DA_i(B)$ .....	$1.07 \pm 0.04$	$2.42 \pm 0.03$	$1.85 \pm 0.01$	$0.96 \pm 0.01$	$0.06 \pm 0.01$	...
$D\phi_{i1}^s(B)$ .....	...	$0.57 \pm 0.20$	$3.21 \pm 0.28$	<u>3.70</u> $\pm 0.67$	$3.35 \pm 0.94$	...
V10 ( $P = 0.775851$ days)						
$A_i(V)$ .....	$0.110 \pm 0.014$	$0.034 \pm 0.001$	$0.013 \pm 0.001$	$0.005 \pm 0.001$	$0.004 \pm 0.001$	$0.002 \pm 0.001$
$A_i(V)$ calc .....	$0.080 \pm 0.001$	$0.057 \pm 0.010$	$0.025 \pm 0.001$	$0.008 \pm 0.001$	$0.001 \pm 0.001$	...
$A_i(B)$ .....	$0.149 \pm 0.003$	$0.049 \pm 0.002$	$0.013 \pm 0.003$	$0.008 \pm 0.003$	$0.004 \pm 0.003$	$0.005 \pm 0.003$
$A_i(B)$ calc .....	$0.124 \pm 0.003$	$0.062 \pm 0.002$	$0.033 \pm 0.002$	$0.008 \pm 0.002$	$0.004 \pm 0.002$	...
$A_{i1}(V)$ .....	$1.00 \pm 0.00$	$0.31 \pm 0.04$	$0.12 \pm 0.02$	$0.05 \pm 0.01$	$0.04 \pm 0.01$	$0.02 \pm 0.01$
$A_{i1}(B)$ .....	$1.00 \pm 0.00$	$0.33 \pm 0.02$	$0.09 \pm 0.02$	$0.05 \pm 0.02$	$0.03 \pm 0.02$	$0.03 \pm 0.02$
$\phi_{i1}^s(V)$ .....	...	$2.64 \pm 0.05$	$5.74 \pm 0.11$	$2.98 \pm 0.29$	$6.15 \pm 0.36$	$3.21 \pm 0.75$
$\phi_{i1}^s(V)$ calc .....	...	$2.90 \pm 0.09$	$5.77 \pm 0.11$	$2.74 \pm 0.25$	$6.00 \pm 0.35$	...
$\phi_{i1}^s(B)$ .....	...	$2.52 \pm 0.06$	$5.44 \pm 0.19$	$1.95 \pm 0.32$	$7.61 \pm 0.60$	$3.09 \pm 0.49$
$\phi_{i1}^s(B)$ calc .....	...	$2.56 \pm 0.11$	$5.32 \pm 0.11$	$3.49 \pm 0.39$	$5.19 \pm 0.29$	...
$DA_i(V)$ .....	$2.93 \pm 0.01$	$2.84 \pm 0.01$	$2.30 \pm 0.01$	$0.86 \pm 0.01$	$1.36 \pm 0.01$	...
$D\phi_{i1}^s(V)$ .....	...	<u>6.55</u> $\pm 0.11$	$0.64 \pm 0.15$	$5.39 \pm 0.39$	$3.12 \pm 0.50$	...
$DA_i(B)$ .....	$2.52 \pm 0.01$	$1.54 \pm 0.01$	$3.85 \pm 0.01$	$0.11 \pm 0.01$	$0.24 \pm 0.01$	...
$D\phi_{i1}^s(B)$ .....	...	$0.98 \pm 0.13$	$2.70 \pm 0.22$	$35.0 \pm 0.5$	<u>48.8</u> $\pm 0.7$	...

TABLE 12  
MEAN  $B-V$  COLORS AND DERIVED  $E(B-V)$  REDDENINGSA. Type  $c$  RR Lyrae Stars

Star (1)	$\log P$ (2)	$\langle B \rangle - \langle V \rangle$		$(B-V)_{\text{mag}}$		$(B-V)_0$ Fourier (SC93, VdB) (7)	$E(B-V)$ (SC93, VdB) mag (8)	$E(B-V)$ CGC(int) (9)
		int (3)	mag (4)	S90 (int) (5)	int+0.007 (6)			
V6.....	-0.5343	0.202	0.202	0.202	0.209	0.187	0.015	...
V7.....	-0.4535	0.207	0.217	0.207	0.214	0.206	0.011	...
V8.....	-0.4403	0.249	0.262	0.250	0.256	0.226	(0.036)	...
V2.....	-0.4214	0.276	0.288	0.276	0.283	0.225	(0.063)	...
Mean ....	-0.4624	0.234	0.242	0.234	0.241	0.211	0.013	...
$\pm$ se .....	0.0249	0.018	0.020	0.018	0.018	0.009	$\pm 0.003$	...

B. Type  $ab$  RR Lyrae Stars

Star (1)	$\log P$ (2)	$\langle B \rangle - \langle V \rangle$		$(B-V)_{\text{mag}}$		$(B-V)_0$ Fourier (J98, K02) (7)	$E(B-V)$ (J98, K02) mag (8)	$E(B-V)$ CGC(int) (J98, K02) (9)
		int (3)	mag (4)	S90 (int) (5)	CGC(int) (6)			
V3.....	-0.2270	0.320	0.343	0.331	0.349	0.353	-0.010	-0.004
V4.....	-0.1758	0.305	0.347	0.348	0.339	0.353	-0.006	-0.014
V1.....	-0.1890	0.334	0.368	0.368	0.358	0.346	0.022	0.012
V9.....	-0.1306	0.365	0.375	0.365	0.379	0.385	-0.010	-0.006
V5.....	-0.1458	0.367	0.380	0.369	0.381	0.386	-0.006	-0.005
V10.....	-0.1102	0.402	0.404	0.402	0.404	0.411	-0.007	-0.007
Mean ....	-0.1631	0.349	0.370	0.364	0.368	0.372	-0.002	-0.004
$\pm$ se .....	0.0174	0.015	0.009	0.015	0.010	0.010	$\pm 0.005$	$\pm 0.004$

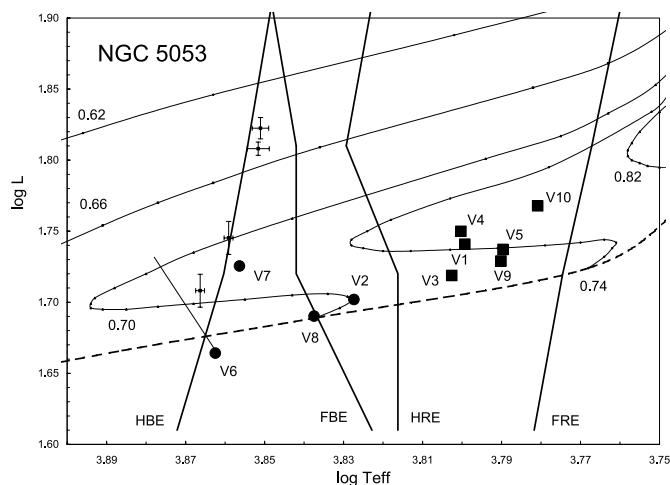


FIG. 9.—H-R diagram showing the NGC 5053 RR Lyrae stars, HB tracks and ZAHB ( $[\text{Fe}/\text{H}] = -2.26$  dex,  $[\text{O}/\text{Fe}] = 0.75$  dex) from Dorman (1992), and theoretical pulsation blue and red edges from Bono et al. (1995). The diagonal line coming off V6 shows the effect of increasing the reddening from  $E(B-V) = 0.0$  to  $0.06$  and would be similar for all the RR Lyrae stars.

$E_{B-V} = 0.06$ , are given in column (7); they are 320–365 K hotter than those derived assuming negligible reddening.

Fourier-based estimates of  $T_{\text{eff}}$  were also calculated for the RRc stars using the relationship given by Simon & Clement (1993):

$$\log T_{\text{eff}} = 3.265 - 0.3026 \log P_H - 0.1777 \log \mathcal{M} + 0.2402 \log L, \quad (7)$$

where  $P_H$  is the first-overtone period for the star, and  $L$  and  $\mathcal{M}$  are in solar units; they are given in the upper half of column (8). The “SC93” equation is based on Ritter’s period-density relation (Schwarzschild 1940), in a form similar to the van Albada & Baker (1971) fundamental equation of stellar

pulsation relating period, mass, luminosity, and temperature. The uncertainties in the resulting  $\log T_{\text{eff}}$  are typically  $\pm 0.002$ , according to the errors in  $\mathcal{M}$ ,  $L$ , and  $P_H$ . The Fourier-based temperatures of V6 and V7 (col. [8]) are  $\sim 100$  K hotter than those derived from the observed mean colors when zero reddening is assumed (col. [6]), but are  $\sim 220$  K cooler than when  $E_{B-V} = 0.06$  was assumed (col. [7]). This finding argues *for* a small amount of reddening and *against* a reddening as great as 0.06.

The Fourier-based temperatures for the RRab stars in column (8) (bottom half) of Table 13 were computed using the two-parameter linear model of Jurcsik (1998):

$$\log T_{\text{eff}} = 3.9291 - 0.1112(V_0 - K_0) - 0.0032[\text{Fe}/\text{H}], \quad (8)$$

where

$$(V_0 - K_0) = 1.585 + 1.257P - 0.273A_1 - 0.234\phi_{31}^5 + 0.062\phi_{41}^5. \quad (9)$$

The temperatures for the RRab stars in column (9) (bottom half) are based on the three-parameter linear model due to Kovács & Walker (1999):

$$\log T_{\text{eff}} = 3.8840 - 0.3219(B - V) + 0.0167 \log g + 0.0070[\text{Fe}/\text{H}]. \quad (10)$$

In both cases the metallicity was assumed to be  $[\text{Fe}/\text{H}] = -2.30$  dex, and in the “KW99” case the  $B-V$  colors were based on the (J98, K02) reddening-free colors (given in the lower half of col. [7] of Table 12) and the Fernie (1995) estimates of surface gravity (col. [3]). In general, the Fourier-based temperatures are consistent with those from the color-temperature relations, with differences between the two sets of estimates ranging from only 8 to 70 K. Comparison of the Fourier-based temperatures with the temperatures computed

TABLE 13  
SURFACE GRAVITIES AND EFFECTIVE TEMPERATURES

A. Type *c* RR Lyrae Stars

STAR (1)	log $P$ (2)	log $g$			log $T_{\text{eff}}$ (mag, VdB)		log $T_{\text{eff}}$ (Fourier)		$E_{B-V} = 0$ (Fourier)	
		F95 (3)	J98 (4)	KW99 (5)	$E_{B-V} = 0$ (6)	$E_{B-V} = 0.06$ (7)	SC93 (8)	— (9)	$\langle \log T_{\text{eff}} \rangle$ (10)	$\langle T_{\text{eff}} \rangle$ (11)
V6.....	−0.5343	3.08	2.97	2.97	3.859	3.878	3.866	...	$3.863 \pm 0.005$	$7286 \pm 91$
V7.....	−0.4535	2.99	2.87	2.88	3.854	3.873	3.859	...	$3.856 \pm 0.004$	$7184 \pm 65$
V8.....	−0.4403	2.98	2.86	2.87	3.837	3.859	(3.851)	...	$3.837 \pm 0.003$	$6878 \pm 80$
V2.....	−0.4214	2.96	2.83	2.84	3.827	3.850	(3.852)	...	$3.827 \pm 0.003$	$6720 \pm 80$

B. Type *ab* RR Lyrae Stars

STAR (1)	log $P$ (2)	log $g$			log $T_{\text{eff}}$ (mag, VdB)		log $T_{\text{eff}}$ (Fourier)		$E_{B-V} = 0$ (Fourier)	
		F95 (3)	J98 (4)	KW99 (5)	$E_{B-V} = 0$ (6)	$E_{B-V} = 0.06$ (7)	J98 (8)	KW99 (9)	$\langle \log T_{\text{eff}} \rangle$ (10)	$\langle T_{\text{eff}} \rangle$ (11)
V3.....	−0.2270	2.88	2.75	2.76	3.805	3.828	3.801	3.803	$3.802 \pm 0.002$	$6348 \pm 28$
V4.....	−0.1758	2.82	2.69	2.71	3.803	3.826	3.797	3.801	$3.800 \pm 0.003$	$6313 \pm 45$
V1.....	−0.1890	2.84	2.66	2.72	3.794	3.818	3.800	3.803	$3.799 \pm 0.005$	$6299 \pm 70$
V9.....	−0.1306	2.77	2.63	2.65	3.791	3.814	3.788	3.792	$3.790 \pm 0.002$	$6168 \pm 30$
V5.....	−0.1458	2.79	2.65	2.67	3.789	3.812	3.790	3.790	$3.790 \pm 0.001$	$6160 \pm 8$
V10.....	−0.1102	2.75	2.61	2.63	3.779	3.804	3.781	3.782	$3.781 \pm 0.001$	$6037 \pm 23$

TABLE 14  
VISUAL ABSOLUTE MAGNITUDES AND DISTANCE MODULUS

A. Type <i>c</i> RR Lyrae Stars									
STAR (1)	PERIOD (days) (2)	$\langle V \rangle_{\text{int}}^0$		$M_V (\mu_V = 16.055)$		$M_V$ (Fourier)		$\mu_0$ (Fourier, $a_V = 0$ )	
		$a_V = 0$ (3)	$a_V = 0.19$ (4)	$a_V = 0$ (5)	$a_V = 0.19$ (6)	K98 (7)	SC93 (8)	K98 (9)	Kin03 (10)
V7.....	0.35194	16.553	16.361	0.498	0.306	0.723	0.442	15.83	15.99
V2.....	0.37896	16.639	16.447	0.584	0.392	0.738	0.294	15.90	16.06
V8.....	0.36284	16.659	16.467	0.604	0.412	0.766	0.259	15.89	16.05
V6.....	0.29219	16.700	16.508	0.645	0.453	0.830	0.526	15.87	16.03

B. Type <i>ab</i> RR Lyrae Stars									
STAR (1)	PERIOD (days) (2)	$\langle V \rangle_{\text{int}}^0$		$M_V (\mu_V = 16.055)$		$M_V$ (Fourier)		$\mu_0$ (Fourier, $a_V = 0$ )	
		$a_V = 0$ (3)	$a_V = 0.19$ (4)	$a_V = 0$ (5)	$a_V = 0.19$ (6)	Kov (7)	Kin03 (8)	Kov (9)	Kin03 (10)
V10.....	0.77585	16.525	16.333	0.470	0.278	0.687	0.538	15.84	15.99
V4.....	0.66707	16.541	16.349	0.486	0.294	0.639	0.476	15.90	16.06
V5.....	0.71487	16.588	16.396	0.533	0.341	0.684	0.534	15.90	16.05
V1.....	0.64717	16.573	16.381	0.518	0.326	0.654	0.485	15.93	16.09
V9.....	0.74022	16.606	16.414	0.551	0.359	0.644	0.481	15.96	16.12
V3.....	0.59295	16.617	16.425	0.562	0.370	0.776	0.617	15.84	16.00

assuming zero reddening (col. [6]) is also informative. The average difference between the “J98” and  $E_{B-V} = 0$  temperatures is only 10 K, and the average  $T_{\text{eff}}$  difference between the KW99 and  $E_{B-V} = 0$  temperatures is only 24 K. Thus, both estimates support negligible reddening rather than  $E_{B-V} = 0.06$ .

Columns (10) and (11) of Table 13 contain the adopted mean values of  $\log T_{\text{eff}}$  and  $T_{\text{eff}}$  and the associated uncertainties (i.e., standard error of the mean). Since the color data clearly favor zero or negligible reddening, only temperatures for which  $E_{B-V} = 0$  was assumed are given. For the RR*ab* stars the  $\log T_{\text{eff}}$  are averages of the values given in columns (6), (8), and (9). Three temperature groups are apparent: the relatively hot stars, V3, V4, and V1; two stars having intermediate temperatures, V9 and V5; and the coolest RR*ab* star, V10. For the RR*c* stars V6 and V7, the temperatures are the averages of columns (6) and (8), while for V8 and V2, the temperatures in column (6) were adopted because the Fourier-based temperatures did not fit any of the standard color-temperature relations.

It is of interest to compare the derived  $T_{\text{eff}}$  with “equilibrium” temperatures computed using equation (16) of Carney et al. (1992):

$$T_{\text{eq}} = 5040 / (0.261 \log P - 0.028A(B) + 0.013[\text{Fe}/\text{H}] + 0.891). \quad (11)$$

Assuming  $[\text{Fe}/\text{H}] = -2.3$  dex and the  $B$  amplitudes given in Table 5, the  $T_{\text{eq}}$  are systematically larger by  $\sim 135$  K than the mean of the  $T_{\text{eff}}$  values given in column (11), with individual differences ranging from +66 to +195 K. Such differences, if real, also favor very low reddening.

## 8. ABSOLUTE MAGNITUDES AND LUMINOSITIES

Sandage et al. (1977) derived a true distance modulus of  $(m - M)_0 = \mu_0 = 16.00$  for NGC 5053, assuming an apparent distance modulus  $\mu_V = 16.03$ , reddening  $E_{B-V} = 0.01 \pm 0.02$ ,

and visual absolute magnitude  $M_V = +0.60$  for the RR Lyrae stars. More recently, Fahlman et al. (1991) derived  $\mu_V = 16.08 \pm 0.05$  from main-sequence fitting and alignment with the fiducial globular cluster M92. The average of these two  $\mu_V$  values, 16.055, has been adopted in the calculations that follow. While the new  $B-V$  colors clearly favor zero (or near-zero) interstellar reddening, the following absolute magnitude and luminosity calculations have been made assuming both  $E_{B-V} = 0.0$  and 0.06.

### 8.1. Visual Absolute Magnitudes

Table 14 contains derived apparent and absolute  $V$  magnitudes and distance moduli. Columns (3) and (4) contain extinction-corrected, intensity-averaged mean apparent  $V$  magnitudes,  $\langle V \rangle_{\text{int}}^0$ , for both cases of reddening, assuming  $a_V = 3.2E_{B-V} = 0.19$  for the visual extinction. The corresponding absolute magnitudes, assuming  $\mu_V = 16.055$  and  $E(B-V) = 0.0$  and 0.06, are given in columns (5) and (6); these illustrate that the  $M_V$  brighten by  $\sim 0.20$  mag when the reddening is assumed to be 0.06.

Absolute magnitudes calculated using Fourier-based equations, and thus independent of the reddening, are given in columns (7) and (8). The  $M_V$  for the RR*c* stars (upper half of col. [7]) were calculated using equation (10) of Kovács (1998):

$$M_V(\text{RRc}) = -0.961P - 4.447A_4 - 0.044\phi_{21}^S + 1.261. \quad (12)$$

The  $M_V$  here is an *intensity*-averaged absolute magnitude,  $A_4$  is the  $V$  amplitude (see Table 9),  $\phi_{21}^S$  is the  $V$  phase difference (see Table 10), and the zero point is on the Baade-Wesselink luminosity scale. Of course, it is important to be aware of the Jurcsik & Kovács (1996) warning that abnormal Fourier coefficients might lead to erroneous  $M_V$  values, and with this in mind we must proceed with caution.

For the RR*ab* stars, the results of two Fourier-based equations for  $M_V$  were averaged and are given in the bottom half of

column (7), where they have been labeled ‘‘Kov.’’ The Kovács & Jurcsik (1996) relation

$$M_V(\text{RR}ab) = -1.396P - 0.477A_1 + 0.103\phi_{31}^s + 1.221 \quad (13)$$

was used to provide one estimate. In this equation, the  $A_1$  are  $V$  amplitudes (Table 9), the  $\phi_{31}^s$  are  $V$  phase differences (Table 11), and again the zero point is fixed by Baade-Wesselink results. The other estimate of  $M_V$  was made using the relation recently derived by Kovács & Walker (2001) and discussed by Kovács (2002):

$$M_V(\text{RR}ab) = -1.876 \log P - 1.158A_1 + 0.821A_3 + \text{const}, \quad (14)$$

where  $A_3$  has been used instead of  $\phi_{31}$ , the standard deviation of the fit to the standard stars was 0.040 mag, and the zero point has been left indeterminate. A constant equal to 0.61 provides consistency with the Kovács & Jurcsik (1996) absolute magnitude scale.

Two recent studies suggest that the Kovács & Jurcsik (1996) and Kovács (1998) luminosity scale may be  $\sim 0.16$  mag too faint. Based on the results of a Fourier analysis of RR Lyrae itself, for which  $M_V = 0.61$  from  $HST$  parallax measurements (Benedict et al. 2002) and  $[\text{Fe}/\text{H}] = -1.4$  dex (Clementini et al. 1995), Kinman et al. (2003) recently reported a value of 0.448 for the constant in equation (14). The  $M_V(\text{RR}ab)$  values computed using this constant are given in the lower half of column (8) in Table 14. They are, on average, 0.16 mag brighter than the Kov values.<sup>4</sup>

Higher luminosities are also predicted by the  $M_V$ - $[\text{Fe}/\text{H}]$  relationship derived by Gratton et al. (2003):

$$M_V(\text{HB}) = (0.22 \pm 0.05)([\text{Fe}/\text{H}] + 1.5) + (0.56 \pm 0.07), \quad (15)$$

which predicts average absolute magnitudes of 0.32, 0.38, and 0.45 (all  $\pm 0.12$ ) for metallicities of  $-2.6$ ,  $-2.3$ , and  $-2.0$  dex, respectively. If this luminosity scale is to be accepted, then either a nonzero reddening or a distance modulus smaller than  $\mu_V = 16.05$  is needed, or the Kovács-Jurcsik scale with a small (or possibly smaller) constant as described by Kinman et al. (2003) should be adopted, or some combination of the these adjustments should be made (depending on the metallicity).

### 8.2. Distance Modulus

The last two columns of Table 14 contain the true distance modulus,  $\mu_0$ , derived for each star using the Fourier-based visual absolute magnitudes,  $M_V$  (col. [7] for the RRc stars and cols. [7] and [8] for the RRab stars) and the observed intensity-averaged magnitudes  $\langle V \rangle_{\text{int}}^0$  given in column (3). The  $\mu_0$  were computed according to

$$\mu_0 = \langle V \rangle_{\text{int}}^0 - M_V. \quad (16)$$

The mean  $\mu_0$  for the RRc stars, computed using the Kovács (1998) expression (upper half of col. [9]), is  $\mu_0 = 15.87 \pm 0.03$ . This mean is nearly identical to that for the RRab stars computed using the Kov average (lower half of

col. [9]),  $15.89 \pm 0.05$ . The mean of these two results gives a true distance modulus of  $\mu_0 = 15.88 \pm 0.03$ , or  $\sim 0.17$  mag smaller than the adopted modulus of 16.055.

On the other hand, using the ‘‘Kinman constant,’’ 0.448, in the Kovács & Walker (2001) equation, gives for the RRab stars (bottom half of col. [10]) a mean  $\mu_0$  of 16.05. In addition, making the  $\mu_0$  for the RRc stars that were derived with the Kovács (1998) formula more distant by 0.16 (the difference between the Kinman constant and the constant needed for consistency of the RRc and RRab results is 0.61) gives for the RRc stars a mean of  $\mu_0 = 16.03$ . Combining these results gives an overall mean of  $\mu_0 = 16.044 \pm 0.013$  for all the RR Lyrae stars, in excellent agreement with the assumed distance modulus of 16.055.

In conclusion, for overall consistency the Kinman constant in the Kovács & Walker (2001) equation for the RRab stars, and the Kovács (1998) equation for the RRc stars with the zero point adjusted from 1.26 to 1.42, seems to provide the most reasonable visual absolute magnitudes and distance moduli.

### 8.3. Bolometric Corrections and Magnitudes

Bolometric corrections for each RR Lyrae star are given in Table 15. These are defined by  $\text{BC} = M_{\text{bol}} - M_V$  and were computed assuming both negligible reddening (col. [3]) and  $E_{B-V} = 0.06$  mag (col. [4]). These corrections are specific for the magnitude-averaged colors given in column (4) of Table 12, i.e.,  $(\langle B \rangle - \langle V \rangle)_{\text{mag}}$ , and are based on the semiempirical BC relation built into the Vandenberg (2000) model for the zero-age HB (ZAHB) in which  $[\text{Fe}/\text{H}] = -2.3$  dex,  $[\alpha/\text{Fe}] = 0.30$  dex, and  $Y = 0.235$ . A second set of BCs for the RRab stars were calculated using the Fourier-based equations given by Jurcsik (1998):

$$\text{BC} = 0.2033 - 0.1736(V-K) + 0.0395[\text{Fe}/\text{H}], \quad (17)$$

where

$$(V-K) = 1.585 + 1.257P - 0.273A_1 - 0.234\phi_{31}^s + 0.062\phi_{41}^s. \quad (18)$$

The latter BCs are similar to the first set of BCs (col. [3]) but are offset by  $\sim 0.02$ . The Vandenberg BCs are also similar to the values derived by Buser & Kurucz (1978) for stars with  $\log g = 2.5$  to 3.0, the latter being  $\sim 0.05$  mag more negative for all values of  $B-V$ .

Table 15 also contains two sets of  $M_{\text{bol}}$ —one set derived assuming, as before,  $\mu_V = 16.055$  and either  $E_{B-V} = 0.0$  or 0.06 (cols. [6]–[7]), and another set (cols. [8]–[9]) derived from the Fourier parameters. All of the  $M_{\text{bol}}$  are based on the  $M_V$  values in Table 14, except for those in the upper half of column (9), which were derived from Fourier-based luminosities (see next section and footnote 4).

### 8.4. Luminosities

Table 16 contains luminosities derived from the  $M_{\text{bol}}$  given in Table 15. They were computed using the well-known relation

$$\log L/L_{\odot} = -0.4(M_{\text{bol}} - M_{\text{bol}\odot}), \quad (19)$$

where  $M_{\text{bol}\odot}$  was assumed to be 4.74, which follows from  $M_{V\odot} = 4.81$  and  $\text{BC}_{\odot} = -0.07$  (see Bessell et al. 1998).

<sup>4</sup> The  $M_V$  values in the upper half of col. [8] were computed from the luminosity equation of Simon & Clement (1993). As has been noted previously, the latter are significantly brighter than the absolute magnitudes computed with the Kovács equation (more so for V2 and V8 than V6 and V7).

TABLE 15  
BOLOMETRIC CORRECTIONS AND ABSOLUTE MAGNITUDES

A. Type <i>c</i> RR Lyrae Stars									
STAR (1)	PERIOD (days) (2)	BC			$M_{\text{bol}} (\mu_V = 16.055)$		$M_{\text{bol}}$ (Fourier)		
		VdB ( $E_{B-V} = 0$ ) (3)	VdB ( $E_{B-V} = 0.06$ ) (4)	Fourier (SC93) (5)	$a_V = 0$ (6)	$a_V = 0.19$ (7)	K98 (8)	SC93 (9)	
V7.....	0.35194	-0.072	-0.047	-0.065	0.426	0.259	0.65	0.38	
V2.....	0.37896	-0.099	-0.076	(-0.074)	0.485	0.316	0.64	0.22	
V8.....	0.36284	-0.089	-0.065	(-0.075)	0.515	0.347	0.68	0.19	
V6.....	0.29219	-0.065	-0.042	-0.056	0.580	0.411	0.77	0.47	

B. Type <i>ab</i> RR Lyrae Stars									
STAR (1)	PERIOD (days) (2)	BC			$M_{\text{bol}} (\mu_V = 16.055)$		$M_{\text{bol}}$ (Fourier)		
		VdB ( $E_{B-V} = 0$ ) (3)	VdB ( $E_{B-V} = 0.06$ ) (4)	Fourier (J98) (5)	$a_V = 0$ (6)	$a_V = 0.19$ (7)	Kov (8)	Kin03 (9)	
V10.....	0.77585	-0.149	-0.119	-0.126	0.321	0.159	0.54	0.39	
V4.....	0.66707	-0.121	-0.099	-0.103	0.365	0.195	0.52	0.36	
V5.....	0.71487	-0.136	-0.110	-0.113	0.397	0.231	0.55	0.40	
V1.....	0.64717	-0.130	-0.106	-0.097	0.388	0.220	0.52	0.36	
V9.....	0.74022	-0.133	-0.108	-0.117	0.418	0.251	0.51	0.35	
V3.....	0.59295	-0.119	-0.097	-0.095	0.443	0.273	0.66	0.50	

Fourier-based luminosities are also given in columns (5) and (6) of Table 16. Simon (1989) first showed that the luminosities (and masses) of RR*c* stars depend primarily on the  $\phi_{31}$  parameter and the first-overtone pulsation period,  $P_H$ , with little dependence on metal abundance. Simon & Clement (1993) later provided the following equation:

$$\log L = 1.04 \log P_H - 0.058 \phi_{31}^s + 2.59, \quad (20)$$

where  $L$  is in solar units and, for the present application,  $\phi_{31}^c$  has been replaced with

$$\phi_{31}^s = \phi_{31}^c + \pi \quad (21)$$

to account for the fact that the Fourier coefficients computed here are based on a sine series and not a cosine series. Substitution of the periods from Table 15 and the  $\phi_{31}^s$  from Table 10 gives the RR*c* luminosities in the upper half of column (6).

## 9. MASSES OF THE RR LYRAE STARS

Masses for the NGC 5053 RR Lyrae stars are also given in Table 16. They were estimated in four ways: (1) by comparing

TABLE 16  
LUMINOSITIES AND MASSES

A. Type <i>c</i> RR Lyrae Stars										
STAR (1)	$\log P_F$ (2)	$\log L/L_{\odot} (\mu_V = 16.055)$		$\log L/L_{\odot}$ (Fourier)		$M/M_{\odot} (\mu_V = 16.055, D92)$		$M/M_{\odot}$ (Fund. Eq.)	$M/M_{\odot}$ (Fourier)	
		$a_V = 0$ (3)	$a_V = 0.19$ (4)	K98 (5)	SC93 (6)	$a_V = 0$ (7)	$a_V = 0.19$ (8)	$a_V = 0$ (9)	SC93 (10)	SC93+D92 (11)
V6.....	-0.4071	1.66	1.73	1.59	1.71	0.68	0.69	0.60	0.68	0.71
V7.....	-0.3263	1.72	1.79	1.64	1.74	0.72	0.65	0.59	0.61	0.70
V8.....	-0.3130	1.69	1.76	1.62	1.82	0.70	0.68	0.65	0.82	0.64
V2.....	-0.2942	1.70	1.77	1.64	1.81	0.70	0.68	0.70	0.73	0.65

B. Type <i>ab</i> RR Lyrae Stars										
STAR (1)	$\log P_F$ (2)	$\log L/L_{\odot} (\mu_V = 16.055)$		$\log L/L_{\odot}$ (Fourier)		$M/M_{\odot} (\mu_V = 16.055, D92)$		$M/M_{\odot}$ (Fund. Eq.)	$M/M_{\odot}$ (Fourier)	
		$a_V = 0$ (3)	$a_V = 0.19$ (4)	Kov (5)	Kin03 (6)	$a_V = 0$ (7)	$a_V = 0.19$ (8)	$a_V = 0$ (9)	SC93 (10)	SC93+D92 (11)
V3.....	-0.2270	1.72	1.79	1.63	1.70	0.72	0.69	0.80	...	...
V1.....	-0.1890	1.74	1.81	1.69	1.75	0.74	0.67	0.77	...	...
V4.....	-0.1758	1.75	1.82	1.69	1.74	0.75	0.66	0.75	...	...
V5.....	-0.1458	1.74	1.80	1.68	1.75	0.74	0.69	0.74	...	...
V9.....	-0.1306	1.73	1.80	1.69	1.76	0.73	0.69	0.68	...	...
V1.....	-0.1102	1.77	1.83	1.68	1.74	0.78	0.66	0.79	...	...

mean locations in an H-R diagram with theoretical HB tracks; (2) by solving for  $\mathcal{M}$  using the fundamental equation of stellar pulsation; and, for the RRc stars only, (3) by using a mass equation based on light-curve Fourier parameters; and (4) by using a hybrid technique involving Fourier-based temperatures and luminosities and interpolation of theoretical HB tracks.

### 9.1. Evolutionary Masses

An H-R diagram of the NGC 5053 RR Lyrae stars is plotted in Figure 9, along with theoretical tracks and blue and red edges of the instability strip. The RRc and RRab stars are represented by solid dots and solid squares, respectively, assuming for both an apparent distance modulus  $\mu_V = 16.055$  and reddening  $E_{B-V} = 0.0$ , thus  $\log T_{\text{eff}}$  is the mean value given in column (10) of Table 13, and  $\log L/L_\odot$  is the value given in column (3) of Table 16. The evolutionary tracks are the low-metallicity, oxygen-enhanced HB models computed by Dorman (1992). The dashed curve is the ZAHB for  $[\text{Fe}/\text{H}] = -2.26$  dex and  $[\text{O}/\text{Fe}] = 0.75$  dex (given in Dorman's Table 2) and the tracks are for five masses 0.62, 0.66, 0.70, 0.74, and 0.82  $\mathcal{M}_\odot$ . The small dots along the tracks correspond to time steps ranging from  $\sim 4$ –5 Myr (for evolution just after the ZAHB) to  $\sim 0.1$  Myr after  $\sim 100$  Myr of evolution. Increasing  $[\text{Fe}/\text{H}]$  by 0.23 dex while decreasing  $[\text{O}/\text{Fe}]$  by 0.05 dex would shift the tracks downward by only 0.01 in  $\log L/L_\odot$ .

All the RR Lyrae stars except V6 have luminosities brighter than the adopted ZAHB. Additional support for the Dorman model comes from the recent calculations of Yi, Lee, & Demarque (1993), which give similar tracks and a ZAHB parallel to, but  $\sim 0.02$  less luminous than the plotted ZAHB, and from the calculations by Pritzl et al. (2002) for which the corresponding ZAHB is  $\sim 0.03$  less luminous. The low-metallicity  $\alpha$ -enhanced ZAHB models of VandenBerg (2000) and VandenBerg et al. (2000), which favor the “short-distance” scale, the Zinn-West metallicity scale, and reconcile synthetic and observed color-magnitude diagrams in the vicinity of the main-sequence turnoff, are  $\sim 0.05$  more luminous than the Dorman models; however, as stated by VandenBerg (2000) “this may simply be an indication that current conductive opacities or the assumed chemical abundance parameters are not quite right.”

The adopted scale is also supported by recent mass calculations for double-mode RR Lyrae (RRd) stars (Kovács 2002), which suggest mass values  $\sim 0.76 \mathcal{M}_\odot$  regardless of the metallicity of the parent cluster. Recent results also suggest that RRd stars have mean luminosities and temperatures midway between the RRc and RRd stars shown in Figure 9 (i.e.,  $\log L \sim 1.72$  and  $\log T_{\text{eff}} \sim 3.82$ ).

Fundamental (F) and first-overtone (H) blue and red edges were derived from the theoretical convective pulsation models of Bono, Caputo, & Marconi (1995). The model edges shown in Figure 9 assume  $M = 0.75 \mathcal{M}_\odot$ ,  $Y = 0.24$ , and  $Z = 0.0001$  and are slightly redder than the  $[\text{Fe}/\text{H}] = -1.93$  dex model edges given by Pritzl et al. (2002). With these values all of the RR Lyrae stars are located between the first-overtone blue edge (HBE) and the fundamental-mode red edge (FRE), the RRc stars lie blueward of the first-overtone red edge (HRE), and the RRab stars lie redward of the fundamental blue edge (FBE), which tend to support the model. As is observed for the RR Lyrae stars in M15 the so-called hysteresis region (the region between the FBE and HRE) for NGC 5053 is populated by RRc stars (in this case, only one RRc star, V2), supporting

the idea that the transition between F and H pulsation occurs near the first-overtone red edge (HRE) in Oo II globular clusters. The absence of RRd stars is probably due to the small population of RR Lyraes.

The masses given in column (7) of Table 16 were estimated by interpolating between the HB tracks in Figure 9. They range from 0.68 to 0.72  $\mathcal{M}_\odot$  for the RRc stars and from 0.72 to 0.78  $\mathcal{M}_\odot$  for the RRab stars, with V6 being the least luminous and V10 the most luminous RR Lyrae star. The masses in column (8) were also derived assuming the temperatures in column (7) of Table 13 and the luminosities in column (4) of Table 16 (derived assuming  $a_V = 0.19$ ). The effect of assuming a high reddening is indicated graphically in Figure 9 by the diagonal line emanating from V6, which also shows how the derived masses would vary with increasing extinction. In general, the masses for the RRc stars change little (i.e., 0.65–0.69  $\mathcal{M}_\odot$ ) with the larger reddening. On the other hand, the derived masses for the RRab stars are significantly lower, the most massive star having a mass of only 0.69 instead of 0.78  $\mathcal{M}_\odot$ . Again however, the temperatures for V6 and V7 would be hotter than expected for RRc stars.

### 9.2. Pulsation Masses

Rearranging the van Albada & Baker (1971) version of the fundamental equation of stellar pulsation provides another way to estimate the mass:

$$\log \mathcal{M} = 1.235 \log L - 1.47 \log P_F - 5.12 \log T_{\text{eff}} + 16.91, \quad (22)$$

where  $L$  and  $\mathcal{M}$  are in solar units. If the temperatures and periods are reasonably well determined and approximately constant, then mass depends chiefly on luminosity, with  $\mathcal{M} \propto L^{1.235}$ . To apply the above equation to the RRc stars, their pulsation periods,  $P_H$ , were converted to the equivalent fundamentalized periods  $P_F$  through the equation

$$\log P_F = \log P_H + 0.1273, \quad (23)$$

where the constant was derived from the mean period ratio of the RRd stars in M15,  $P_H/P_F = 0.7460$  (Nemec 1985). Values of  $\log P_F$  are given in column (2) of Table 16, and the derived masses are given in column (9). The latter agree with masses based on the interpolated HB tracks (col. [7]) only for half the stars (V1, V2, V4, V5, and V10). For the remaining stars, the pulsation masses tend to be smaller than the evolutionary masses. Increasing the reddening reduces the differences but has already been ruled out by temperature considerations.

### 9.3. Fourier-based Masses

Masses for the RRc stars were also computed using the mass equation derived by Simon & Clement (1993). Since the Fourier phase differences were based on a sine (and not cosine) series,  $\phi_{31}^c$  of SC93 was replaced with  $\phi_{31}^s = \phi_{31}^c + \pi$ , therefore, the following mass equation was used:

$$\log \mathcal{M}/\mathcal{M}_\odot = 0.52 \log P_H - 0.11 \phi_{31}^s + 0.74. \quad (24)$$

With this equation, the derived masses (col. [10] of Table 16) range from  $0.61 \pm 0.03 \mathcal{M}_\odot$  (V7) to  $0.82 \pm 0.04 \mathcal{M}_\odot$  (V8), where the uncertainties were obtained by propagation of the errors in the phase parameters.

TABLE 17  
METAL ABUNDANCES FOR THE RR*ab* STARS

Star	$P$ (days)	Filter	$D_m$ (JK)	$D_m$ (KK)	[Fe/H]
(1)	(2)	(3)	(4)	(5)	(6)
V3.....	0.59295	$V$	$5.31 \pm 0.19$	4.74	$-1.54 \pm 0.07$
V1.....	0.64717	$V$	$4.18 \pm 0.01$	2.83	$-1.72 \pm 0.06$
V4.....	0.66707	$V$	$0.88 \pm 0.01$	0.89	$-1.85 \pm 0.06$
V5.....	0.71487	$V$	$4.40 \pm 0.44$	1.52	$-1.64 \pm 0.10$
V9.....	0.74022	$V$	$1.93 \pm 0.41$	1.55	$-1.70 \pm 0.11$
V10.....	0.77585	$V$	$6.55 \pm 0.11$	5.15	$-1.51 \pm 0.16$

#### 9.4. Hybrid Masses

A final set of mass estimates for the RR*c* stars was based on the Dorman tracks and the  $T_{\text{eff}}$  and  $\log L$  calculated using the Simon & Clement (1993) equations (see Tables 13 and 16). These “hybrid” masses are recorded in column (11) of Table 16. Notice that in the color-magnitude diagram, the assumed locations of the four RR*c* stars (which are plotted in Fig. 9 as small dots with error bars) are near the HBE line. Moreover, although the locations of V6 and V7 are close to their solid dot counterparts, V8 and V2 are much more luminous. In addition, the Fourier-based  $T_{\text{eff}}$  range is noticeably smaller than that implied by the observed colors and is, in fact, unreasonably small; a similar conclusion concerning the Simon & Clement (1993) equations was reached by Kovács (1998). In general, the hybrid masses are significantly different from those derived using the Fourier-based mass equation (compare cols. [10] and [11] of Table 16). The only (approximate) agreement is for V6; for V8, the mass equation gives  $\mathcal{M} = 0.82 \mathcal{M}_{\odot}$  (the highest mass for the four stars) while the HB tracks suggest mass =  $0.64 \mathcal{M}_{\odot}$ , the lowest of the four masses; and, the disagreement in mass for both V7 and V2 is  $\sim 0.10 \mathcal{M}_{\odot}$ .

#### 10. METAL AND HELIUM ABUNDANCES

According to the Zinn & West (1984) catalog of globular cluster properties, NGC 5053 is the most metal-poor globular cluster in our Galaxy, with individual stars having an iron to hydrogen ratio  $[\text{Fe}/\text{H}] = -2.58 \pm 0.27$  dex (i.e., approaching 1/400th that of the Sun). The more recent on-line compilation by Harris (1996) identifies the five most metal-poor galactic globular clusters as NGC 5053 ( $-2.29$  dex), M92 ( $-2.29$  dex), NGC 6426 ( $-2.26$  dex), M15 ( $-2.25$  dex), and NGC 5466 ( $-2.22$  dex). These two studies raise an important question concerning the metallicity of NGC 5053: is its  $[\text{Fe}/\text{H}]$  significantly lower or identical to that of other very low metallicity globular clusters in our Galaxy (i.e.,  $-2.6$  or  $-2.3$  dex)?

Recent reviews of the metallicity of NGC 5053 are given by Sarajedini & Milone (1995) and Sohn (2001). These authors present their own findings based on a “simultaneous reddening and metallicity” method using  $B-V$  and  $V-I$  colors, Sarajedini & Milone deriving  $[\text{Fe}/\text{H}] = -2.41 \pm 0.10$  dex and Sohn finding  $[\text{Fe}/\text{H}] = -2.62 \pm 0.07$  dex or  $-2.50$  dex using a similar approach. The very long mean period of the RR*ab* stars,  $\langle P_{ab} \rangle = 0.6897$ , which is the longest of any known Oosterhoff type II globular cluster, the locations of the 10 RR Lyrae stars in a period-amplitude diagram (i.e., long periods for a given amplitude, like the RR Lyraes in M15), and the extremely short periods of the SX Phe stars (Nemec et al. 1995), all favor a very low metallicity for NGC 5053. Unfortunately, all of these estimates lack the necessary precision to answer the above question.

#### 10.1. Fourier-based $[\text{Fe}/\text{H}]$ for the RR*ab* Stars

In principle, Fourier decomposition of the RR Lyrae light curves provides another method for estimating  $[\text{Fe}/\text{H}]$ . The following relation was derived by Jurešik & Kovács (1996) for the metal abundances of individual RR*ab* stars in globular clusters:

$$[\text{Fe}/\text{H}] = -5.038 - 5.394P + 1.345\phi_{31}^s. \quad (25)$$

In this equation,  $\phi_{31}^s$  was derived from  $V$  light curves, and the root mean square error of the overall fit was 0.13 dex. The authors recommended that application of this equation be limited to stars with  $D_m$  less than 3, where  $D_m$  is the maximum of the deviation parameters for the nine quantities  $A_1$  to  $A_5$  and  $\phi_{21}$  to  $\phi_{51}$ . Equations for computing the uncertainty in the predicted  $[\text{Fe}/\text{H}]$  values also were provided.

Metal abundances for the NGC 5053 RR*ab* stars derived using the above method are presented in Table 17. The uncertainties are values propagated from the errors in  $P$  and  $\phi_{31}^s$  (given in Table 11). Only two of the six stars (V4 and V9) have  $D_m < 3$  and for these the mean  $[\text{Fe}/\text{H}]$  equals  $-1.78$  dex. Relaxing the JK selection criterion to  $D_m < 5$ , or using the Kovács & Kanbur (1998)  $D_m < 3$  values (col. [5] of Table 17), increases the number of qualifying light curves to four with a mean  $[\text{Fe}/\text{H}] = -1.73$  dex. If the current calibration is considered to be reliable, then both cases suggest that the mean metallicity is significantly richer than either  $-2.3$  or  $-2.6$  dex. However, this seems unlikely. In their original paper Jurešik & Kovács (1996) pointed out that their formula overestimates  $[\text{Fe}/\text{H}]$  for metal poor clusters, in particular M68 and M92. More recently, Schwarzenberg-Czerny & Kaluzny (1998) and Kovács (2002) have also suggested that the Fourier parameter-based  $[\text{Fe}/\text{H}]$  calibration should be revised downward by  $\sim 0.3$  dex for RR Lyraes with very low metal abundances. The present results not only support this conclusion but might even argue for a larger downward revision.

#### 10.2. (Relative) Helium Abundances for the RR*c* Stars

In their analysis of the Fourier parameters of RR*c* stars, Simon & Clement (1993) introduced a parameter, denoted  $Y$ , which was conjectured to be a measure of the relative helium abundance:

$$\log Y = -20.26 + 4935 \log T_{\text{eff}} - 0.2638 \log \mathcal{M} + 0.3318 \log L. \quad (26)$$

Computed values of  $Y$  for V6, V7, V8, and V2 are 0.27, 0.26, 0.24, and 0.24, respectively, with formal uncertainties of  $\pm 0.01$ . The values for V6 and V7 are similar to those derived for other globular clusters—for example,  $Y = 0.266$  for M9

(Clement & Shelton 1999) and  $Y = 0.27 \pm 0.01$  for M55 (Olech et al. 1999). The low values for V8 and V2 may be spurious, reflecting problems related to their Fourier-derived temperatures.

## 11. SUMMARY

The pulsation characteristics of the RR Lyrae stars in the very metal poor globular cluster NGC 5053 have been derived using new  $B$  and  $V$  CCD photometry acquired since 1994. With the derivation of  $P = 0.7585$  days for V10, periods accurate to  $\lesssim 10^{-5}$  days are now known for all 10 variable stars. Mean magnitudes, colors, amplitudes, and Fourier coefficients were also derived from new high-precision light curves.

Using available times of maximum light dating back to Baade's original 1923–1927 observations, accurate period change rates were obtained. These indicate that seven of the 10 stars have increasing periods and three have decreasing periods. Taking into account the uncertainties in the estimated  $dP/dt$ , a constant period cannot be ruled out for the four most slowly varying stars. The measured mean period change rate,  $0.04 \pm 0.04$  days  $\text{Myr}^{-1}$ , is consistent with Young-Wook Lee's evolutionary model predictions for a globular cluster with HB type  $\sim 0.5$ .

Mean  $B-V$  colors were found to range from 0.20 to 0.40 and are consistent with zero or near-zero reddening, as first suggested by Sandage et al. (1977). In addition, a reddening  $E_{B-V} = 0.018 \pm 0.003$  was derived from the recent SFD maps. Both results tend to rule out the more recent suggestions that  $E_{B-V} = 0.06$ . Mean effective temperatures vary from 6040 K (V10) to 7290 K (V6), with  $\log g$  in the range 2.6–3.1. Depending on the assumptions, visual absolute magnitudes range from  $M_V = 0.25$  to 0.83, with the most probable mean value for the ensemble of RR Lyrae stars being 0.55. Luminosities were derived assuming a distance modulus  $\mu_V = 16.055$  and the limiting reddening cases of  $E_{B-V} = 0.0$  and 0.06. The resulting estimates for zero reddening are comparable to luminosities derived from the Fourier-based equations. Mean locations of the stars in the H-R diagram show a clear progression from hot low- $L$  stars to cool high- $L$  stars and are consistent with the theoretical blue and red edges of the instability strip calculated by Bono et al. (1995). The most probable estimated masses for the 10 stars, obtained by comparison with the Dorman HB models, range from  $0.68 M_\odot$  (V6) to  $0.78 M_\odot$  (V10).

Finally, metal abundances were derived using the method developed by Jurcsik & Kovács (1996) and were found to be significantly higher than the mean determined using other more well established measures. This supports recent suggestions that the Fourier-based  $[\text{Fe}/\text{H}]$  calibration may need to be reduced by at least 0.3 for very low metal abundance clusters.

I wish to thank International Statistics and Research Corporation for financial support, and I am grateful to the Dominion Astrophysical Observatory time allocation committees for generous awards of observing time on the 1.8 m (72 inch) Plaskett telescope. Geza Kovács and Siobahn Morgan kindly sent me their Fourier decomposition programs, Don Vandenberg sent his most recent ZAHB models, and Ben Dorman provided early drafts of his papers. I also thank the anonymous referee for useful suggestions that helped to improve the paper. Finally, the period change rate study was possible only because Walter Baade, Helen Sawyer,

Leonida Rosino, and Giuseppe Mannino had the foresight to publish the details of their photometry and the times of their observations.

## APPENDIX

### NOTES ON INDIVIDUAL STARS

This section contains detailed notes on the RR Lyrae stars in NGC 5053. The abbreviations  $P_S$ ,  $P_R$ , and  $P_M$  are used to denote the pulsation periods determined by Sawyer (1946), Rosino (1949) and Mannino (1963).

**V1:** The photometry since 1995 shows significant year-to-year and within-year shifts, with possible periodic variations. Continued high-precision observations are desirable.

**V2:** There are not yet enough observations to be able to distinguish between the constant period,  $P = 0.3789536 \pm 0.0000002$  days, or a very slowly increasing period,  $dP/dt = 0.01 \pm 0.02$  days  $\text{Myr}^{-1}$ .

**V3:** Small cycle-to-cycle variations are seen in the light-curve shape, in particular the 2001  $V$  photometry. The phase at maximum light is smoothly shifting (Fig. 5) suggesting a slowly increasing period,  $dP/dt = 0.09$  days  $\text{Myr}^{-1}$ , rather than a constant period.

**V4:** Although this RRab star is crowded by a close neighbor the light curve is surprisingly well defined. In fact, its  $D_m(V)$  value (0.88) is the smallest of the six RRab stars, and  $D_m(B)$  (3.24) is the second smallest (behind 2.73 for V3).

**V5:** The new photometry shows a shoulder in the  $B$  and  $V$  light curves, most clearly seen in the 2001–2002 photometry. To model this shoulder, 15 Fourier terms were needed for the  $V$  data. Owing to fewer data points, only seven terms were needed to model the  $B$  photometry. The small  $p$ -value (0.001) for the “ $c$ ” coefficient suggests that the quadratic fit is to be preferred over the linear fit. Note that there is a typographical error in the “Notes on Individual Stars” section of the paper by Nemeč et al. (1995).

**V6:** A relatively flat top is observed in the light curve at maximum light, with the possibility of a double bump. The significant period change rate is well determined.

**V7:** Mannino (1963) concluded that the period is increasing, at the rate  $\beta = +0.50$  days  $\text{Myr}^{-1}$ . A reanalysis of the photometry available to Mannino, adopting the phase shifts that he would have assumed, confirms that one might conclude that  $P$  is increasing, not at the rate  $+0.50$  but at  $+0.75$  days  $\text{Myr}^{-1}$ ; including the photometry since 1986 gives an even-faster period change rate of  $+0.95 \pm 0.10$  days  $\text{Myr}^{-1}$ . The difficulty with this solution is that it predicts a period for the current epoch (2000–2002) of 0.351974 days, which differs considerably from period search results. In addition, the phase-shift diagram shows that the newer photometry deviates from the predicted phase shifts by more than  $3\sigma$  (see Fig. 5). Thus, a rapidly increasing period is rejected in favor of the solution given in Table 7 (i.e., a period that is changing at the rate  $dP/dt = -0.28 \pm 0.04$ ). In the latter case, the predicted period for the current epoch is the more probable value  $P = 0.351931$  days. Both the  $V$  and  $B$  light curves show a clear dip just before maximum light (see Fig. 2). Further accurate photometry is needed to be sure of the period change rate.

**V8:** Both Sawyer and Mannino concluded that the period is decreasing at the rate  $\beta \sim 1.1 \times 10^{-9}$  (i.e.,  $dP/dt = -0.40$  days  $\text{Myr}^{-1}$ ). With the new photometry, it is easy to see why this

conclusion was reached: if the “phase at maximum light” from Baade’s 1923–1927 data is assumed to be  $-2.6$  instead of  $-1.6$ , then a decreasing period follows. However, the 1986–2002 data indicate that the period is increasing. Adopting  $P_M$  as the starting point,  $dP/dt$  was found to be  $+0.54$  days  $\text{Myr}^{-1}$ . This period change rate predicts that the period expected for the 1997–2002 epoch is near  $0.362868$  days. A period search of the  $V$  photometry for the 1997–2002 epoch confirms this period. The Fourier decomposition and the 1999–2002 light curve (which has a standard deviation of  $0.038$  mag) suggests the possibility of slight variations from month to month.

**V9:** The real-time light curves based on extensive photometry since 1995, and the red color of the star, support the long period first identified by Mannino,  $P_M = 0.7402201$  days. The phase-shift diagram (Fig. 5) based on  $P_M$  with an epoch of maximum light  $T_0 = 2,437,371.407$  suggests that the period is either constant at  $0.7402195$  days, or increasing at the very slow rate,  $dP/dt = 0.05 \pm 0.05$  days  $\text{Myr}^{-1}$ . The light curves exhibit considerable scatter ( $\sigma_V = 0.038$  mag,  $\sigma_B = 0.076$  mag).

**V10:** The period is either changing very slowly at a rate estimated to be  $-0.03 \pm 0.07$  days  $\text{Myr}^{-1}$ , or is constant with the value  $0.7758485 \pm 0.0000004$  days.

## REFERENCES

- Baade, W. 1928, Mitt. Hamburger, Sternwarte, B6, 29  
 Benedict G. F., et al. 2002, AJ, 123, 473  
 Bessell, M. S., Castelli, F., & Plez, B. 1998, A&A, 333, 231  
 Bono, G., Caputo, F., & Marconi, M. 1995, AJ, 110, 2365  
 Buser, R., & Kurucz, R. L. 1978, A&A, 70, 555  
 Carney, B. W., Storm, J., & Jones, R. V. 1992, ApJ, 386, 663  
 Carretta, E., Gratton, R. G., & Clementini, G. 2000, MNRAS, 316, 721  
 Clement, C. M., & Rowe, J. 2000, AJ, 120, 2579  
 Clement, C. M., & Shelton, I. 1999, AJ, 118, 453  
 Clementini, G., Carretta, E., Gratton, R., Merighi, R., Mould, J. R., & McCarthy, J. K. 1995, AJ, 110, 2319  
 Corwin, T. M., Catelan, M., Smith, H. A., Borissova, J., Ferraro, F. R., & Raburn, W. S. 2003, AJ, 125, 2543  
 Dorman, B. 1992, ApJS, 81, 221  
 Fahlman, G. G., Richer, H., & Nemeč, J. 1991, ApJ, 380, 124  
 Fernie, D. 1995, AJ, 110, 2361  
 Gratton, R. G., Bragaglia, A., Carretta, E., Clementini, G., Desidera, S., Grundahl, F., & Lucatello, S. 2003, A&A, 408, 529  
 Harris, W. E. 1996, AJ, 112, 1487  
 Iben, I., Jr., & Rood, R. T. 1970, ApJ, 161, 587  
 Jurcsik, J. 1998, A&A, 333, 571  
 Jurcsik, J., & Kovács, G. 1996, A&A, 312, 111  
 King, I. 1962, AJ, 67, 471  
 Kinman, T., Bragaglia, A., Cacciari, C., Buzzoni, A., & Spagna, A. 2003, preprint  
 Kovács, G. 1998, Mem. Soc. Astron. Italiana, 69, 49  
 ———. 2002, in ASP Conf. Ser. 265,  $\omega$  Centauri: Unique Window into Astrophysics, ed. F. van Leeuwen, J. Hughes, & G. Piotto (San Francisco: ASP), 163  
 Kovács, G., & Jurcsik, J. 1996, ApJ, 466, L17  
 Kovács, G., & Kanbur, S. M. 1998, MNRAS, 295, 834  
 Kovács, G., & Walker, A. R. 1999, ApJ, 512, 271  
 ———. 2001, A&A, 371, 579  
 Laffer, J., & Kinman, T. 1965, ApJS, 11, 216  
 Lee, Y.-W. 1990, ApJ, 363, 159  
 ———. 1991, ApJ, 367, 524  
 Lee, Y.-W., Demarque, P., & Zinn, R. 1994, ApJ, 423, 248  
 Mannino, G. 1963, Publ. Obs. Bologna, 8, 12  
 Nemeč, J. M. 1985, AJ, 90, 240  
 Nemeč, J. M., & Cohen, J. G. 1989, ApJ, 336, 780  
 Nemeč, J. M., Hazen-Liller, M., & Hesser, J. E. 1985, ApJS, 57, 329  
 Nemeč, J. M., Linnell Nemeč, A. F., & Lutz, T. E. 1994, AJ, 108, 222  
 Nemeč, J. M., & Mateo, M. 1990, in ASP Conf. Ser. 11, Confrontation Between Stellar Pulsation and Evolution, ed. C. Cacciari & G. Clementini (San Francisco: ASP), 64  
 Nemeč, J. M., Mateo, M., Burke, M., & Olszewski, E. W. 1995, AJ, 110, 1186  
 Nemeč, J. M., Mateo, M., & Schombert, J. M. 1995, AJ, 109, 618  
 Olech, A., Kaluzny, J., Thompson, I. B., Pych, W., Krzeminski, W., & Schwarzenberg-Czerny, A. 1999, AJ, 118, 442  
 ———. 2001, MNRAS, 321, 421  
 Petersen, J. O. 1986, A&A, 170, 59  
 Preston, G. W. 1961, ApJ, 133, 29  
 Pritzl, B. J., Smith, H. A., Catelan, M., & Sweigart, A. V. 2002, AJ, 124, 949  
 Rosino, L. 1949, Mem. Soc. Astron. Italiana, 20(3), 227  
 Sandage, A. R. 1990, ApJ, 350, 603  
 Sandage, A. R., Katem, B., & Johnson, H. 1977, AJ, 82, 389  
 Sarajedini, A., & Milone, A. A. E. 1995, AJ, 109, 269  
 Sawyer, H. 1946, Pub. David Dunlap Obs. 1(18), 357  
 Schlegel, D. J., Finkbeiner, D. P., & Davis, M. 1998, ApJ, 500, 525  
 Schwarzenberg-Czerny, A., & Kaluzny, J. 1998, MNRAS, 300, 251  
 Schwarzschild, M. 1940, Harvard Circ., No. 437  
 Simon, N. R. 1989, ApJ, 343, L17  
 Simon, N. R., & Clement, C. M. 1993, ApJ, 410, 526  
 Simon, N. R., & Lee, A. S. 1981, ApJ, 248, 291  
 Smith, H. 1995, RR Lyrae Stars (Cambridge: Cambridge Univ. Press)  
 Smith, H. A., & Sandage, A. 1981, AJ, 86, 1870  
 Sohn, Y.-J. 2001, J. Astron. Space Sci., 18(1), 7  
 Stagg, C., & Wehlau, A. 1980, AJ, 85, 1182  
 Stellingwerf, R. F., & Donohoe, M. 1986, ApJ, 306, 183  
 Stetson, P. B. 1987, PASP, 99, 191  
 van Albada, T. S., & Baker, N. 1971, ApJ, 169, 311  
 VandenBerg, D. A. 2000, ApJS, 129, 315  
 VandenBerg, D. A., & Clem, J. L. 2003, AJ, 126, 778  
 VandenBerg, D. A., Swensen, F. J., Rogers, F. J., Iglesias, C. A., & Alexander, D. R. 2000, ApJ, 532, 430  
 Wehlau, A., Slawson, R. W., & Nemeč, J. M. 1999, AJ, 117, 286  
 Yi, S., Lee, Y.-W., & Demarque, P. 1993, ApJ, 411, L25  
 Zinn, R., & West, M. J. 1984, ApJS, 55, 45